

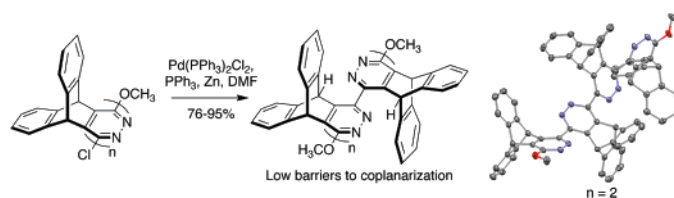
Iptycene-Derived Pyridazines and Phthalazines

Jean Bouffard, Robert F. Eaton,[†] Peter Müller, and Timothy M. Swager*

Department of Chemistry, Massachusetts Institute of Technology, 77 Massachusetts Avenue, Cambridge, Massachusetts 02139

tswager@mit.edu

Received September 12, 2007



The synthesis of new heterocyclic oligo(phenylene) analogues based on soluble, nonaggregating 1,2-diazines is reported. Improved palladium-catalyzed reductive coupling methods were developed to allow for the preparation of large quantities of iptycene-derived bipyridazines and biphthalazines, and the controlled synthesis of well-defined oligomers up to sexipyridazine. Crystallographic, spectroscopic, and computational evidence indicate that in these analogues, hindrance at the ortho position is relaxed relative to poly(phenylenes). The resulting building blocks are promising for incorporation in conjugated electronics materials, and as new iptycene-derived ligands for transition metals.

Introduction

Molecules of the iptycene family, as exemplified by their simplest member triptycene, have been the object of much interest by numerous research groups, including our own. In particular, iptycenes have been incorporated in organic materials and polymers for applications that include conjugated polymer sensors,¹ high mechanical performance polymers,² liquid crystals,³ low- κ dielectrics,⁴ gas absorption/storage,⁵ and host-guest chemistry.⁶ In the bulk of these examples, the introduction of molecular voids, or internal free volume, has been proposed to be at the origin of the exceptional materials properties. By contrast, only a few heterocyclic members of the iptycene family

have been prepared and explored for materials applications. Iptycene-derived thiophenes and pyrroles have been incorporated in conjugated polymers,⁷ porphyrins,⁸ phthalocyanines,⁹ and related macrocycles.¹⁰ Iptycene-derived pyridines have also been reported¹¹ but, to the best of our knowledge, have yet to be

[†] Deceased.

(1) (a) Yang, J.-S.; Swager, T. M. *J. Am. Chem. Soc.* **1998**, *120*, 5321–5322. (b) Yang, J.-S.; Swager, T. M. *J. Am. Chem. Soc.* **1998**, *120*, 11864–11873.

(2) (a) Tsui, N. T.; Paraskos, A. J.; Torun, L.; Swager, T. M.; Thomas, E. L. *Macromolecules* **2006**, *39*, 3350–3358. (b) Tsui, N. T.; Torun, L.; Pate, B. D.; Paraskos, A. J.; Swager, T. M.; Thomas, E. L. *Adv. Funct. Mater.* **2007**, *17*, 1595–1602.

(3) (a) Long, T. M.; Swager, T. M. *J. Mater. Chem.* **2002**, *12*, 3407–3412. (b) Norvez, S. *J. Org. Chem.* **1993**, *58*, 2414–2418.

(4) Long, T. M.; Swager, T. M. *J. Am. Chem. Soc.* **2003**, *125*, 14113–14119.

(5) Ghanem, B. S.; Msayib, K. J.; McKeown, N. B.; Harris, K. D. M.; Pan, Z.; Budd, P. M.; Butler, A.; Selbie, J.; Book, D.; Walton, A. *Chem. Commun.* **2007**, 67–69.

(6) (a) Han, T.; Zong, Q.-S.; Chen, C.-F. *J. Org. Chem.* **2007**, *72*, 3108–3111. (b) Peng, X.-X.; Lu, H.-Y.; Han, T.; Chen, C.-F. *Org. Lett.* **2007**, *9*, 895–898 and references therein.

(7) (a) Williams, V. E.; Swager, T. M. *Macromolecules* **2000**, *33*, 4069–4073. (b) Tsai, Y. C.; Davis, J.; Compton, R. G.; Ito, S.; Ono, N. *Electroanalysis* **2001**, *13*, 7–12 and references therein.

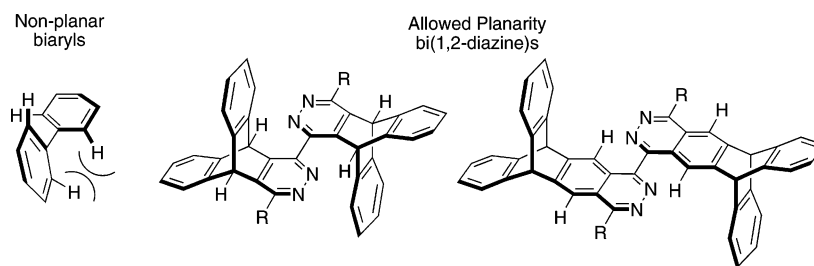
(8) (a) Uno, H.; Watanabe, H.; Yamashita, Y.; Ono, N. *Org. Biomol. Chem.* **2005**, *3*, 448–453. (b) Schwenninger, R.; Schögl, J.; Maynollo, J.; Gruber, K.; Ochsenein, P.; Bürgi, H.-B.; Konrat, R.; Kräutler, B. *Chem. Eur. J.* **2001**, *7*, 2676–2686. (c) Schwenninger, R.; Ramondenc, Y.; Wurst, K.; Schögl, J.; Kräutler, B. *Chem. Eur. J.* **2000**, *6*, 1214–1223. (d) Ramondenc, Y.; Schwenninger, R.; Phan, T.; Gruber, K.; Kratky, C.; Kräutler, B. *Angew. Chem. Int. Ed.* **1994**, *33*, 889–891.

(9) (a) Oliver, S. W.; Smith, T. D. *J. Chem. Soc. Perkin Trans. II* **1987**, 1579–1582. (b) Kopranenkov, V. N.; Rummyantseva, G. I.; Luk'yanets, E. A. *Zh. Obshch. Khim.* **1972**, *42*, 2586. (c) Kopranenkov, V. N.; Rummyantseva, G. I. *Zh. Obshch. Khim.* **1975**, *45*, 1555–1559. (d) Gal'pern, M. A.; Shalaev, V. K.; Shatskaya, T. A.; Shishkanova, L. S.; Skvarchenko, V. R.; Luk'yanets, E. A. *Zh. Obshch. Khim.* **1983**, *53*, 2601–2606. (e) Shatskaya, T. A.; Gal'pern, M. G.; Skvarchenko, V. R.; Luk'yanets, E. A. *Zh. Obshch. Khim.* **1986**, *56*, 392–397.

(10) (a) Tomé, J. P. C.; Cho, D.-G.; Sessler, J. L.; Neves, M. G. P. M. S.; Tomé, A. C.; Silva, A. M. S.; Cavaleiro, J. A. S. *Tetrahedron Lett.* **2006**, *47*, 3131–3134. (b) Silva, A. M. G.; Tomé, A. C.; Neves, M. G. P. M. S.; Cavaleiro, J. A. S.; Kappe, C. O. *Tetrahedron Lett.* **2005**, *46*, 4723–4726.

(11) (a) Skvarchenko, V. R.; Koshkina, N. P. *Zh. Org. Khim.* **1979**, *15*, 2367–2370. (b) Skvarchenko, V. R.; Koshkina, N. P.; Abramov, A. V. *Zh. Org. Khim.* **1981**, *17*, 1018–1023. (c) Skvarchenko, V. R.; Koshkina, N. P. *Zh. Org. Khim.* **1982**, *17*, 2410–2414. (d) Skvarchenko, V. R.; Lapteva, V. L.; Gorbunova, M. A. *Zh. Org. Khim.* **1990**, *26*, 2588–2590.

SCHEME 1



elaborated into larger functional molecules or assemblies. We are aware of three reports of iptycene-derived pyridazines,¹² but details regarding their preparation, characterization, and properties are scarce. In this paper, we present the synthesis and characterization of iptycene-derived pyridazines and phthalazines, and their elaboration into building blocks for materials applications.

Results and Discussion

Design Considerations. Our interest in the development of 1,2-diazine-derived building blocks for materials applications spawned from three principal design considerations. First, electron-poor building blocks can confer a number of attractive characteristics, including resistance to photooxidation¹³ and a lowered barrier to electron injection (n-doping),¹⁴ which can translate to devices operating at lower voltages and with extended lifetimes. Second, as part of a long-standing interest toward the control of conformation in conjugated polymers,¹⁵ we hypothesized that when compared to the analogous poly(phenylene)s bearing hydrogens in ortho positions, poly(1,2-diazine)s would exhibit less steric hindrance and would favor, with potential hydrogen bonding, planarization and therefore more extended π -conjugation¹⁶ (Scheme 1). Consequently, iptycene-derived poly(1,2-diazine)s could exhibit a fully coplanar conjugated backbone, yet remain soluble due to the limited propensity of iptycene-derived molecules to aggregate and π -stack in the solid state. Third and finally, we can exploit the

coordination sites of the heterocyclic nitrogen atoms¹⁷ for the preparation of metal-containing materials and polymers, with a special interest for design of phosphorescent conjugated polymers for lighting and sensing applications.^{18,19}

Synthesis of Iptycene-Derived Pyridazines. Our initial synthetic approach focused on the Diels–Alder cycloaddition between anthracene and dimethylacetylene dicarboxylate (DMAD),²⁰ followed by treatment with hydrazine and halogenation with a phosphorus(V) halide. However, as indicated in a previous report,²¹ treatment of the adduct **1a** with hydrazine under various reaction conditions exclusively afforded the reduced 5-membered *N*-aminoimide **7** (Scheme 2). Following the procedure of Mizzoni and Spoerri,²² reaction of the bicyclic maleic anhydride **3a**, obtained from the adduct **1a** after saponification with sodium hydroxide and dehydration with oxalyl chloride, with hydrazine monohydrochloride in refluxing acetic acid afforded the desired 6-membered cyclic hydrazide **4a** in excellent yields. Treatment with neat phosphorus oxychloride or molten phosphorus oxybromide afforded the dihalides **5a,d** in good yields. Due to the high cost of phosphorus oxybromide and the requirement of several equivalents of the reagent for a reaction in the melt, large-scale preparation of the dibromide may benefit from the alternate use of phosphorus pentoxide and tetra-*n*-butylammonium bromide in toluene,²³ a

(17) For examples of pyridazine-based metal complexes: (a) Plasseraud, L.; Maid, H.; Hampel, F.; Saalfrank, R. W. *Chem. Eur. J.* **2001**, *7*, 4007–4011. (b) Slater, J. W.; Lyndon, D. P.; Alcock, N. W.; Rourke, J. P. *Organometallics* **2001**, *20*, 4418–4423. (c) Marquis, A.; Kintzinger, J.-P.; Graff, R.; Baxter, P. N.; Lehn, J.-M. *Angew. Chem., Int. Ed.* **2002**, *41*, 2760–2764 and references cited therein.

(18) (a) Thomas, S. W., III; Venkatesan, K.; Müller, P.; Swager, T. M. *J. Am. Chem. Soc.* **2006**, *128*, 16641–16648. (b) Thomas, S. W., III; Yagi, S.; Swager, T. M. *J. Mater. Chem.* **2005**, *15*, 2829–2835. (c) Sandee, A. J.; Williams, C. K.; Evans, N. R.; Davies, J. E.; Boothby, C. E.; Köhler, A.; Friend, R. H.; Holmes, A. B. *J. Am. Chem. Soc.* **2004**, *126*, 7041–7048. (d) Liu, S.-J.; Zhao, Q.; Deng, Y.; Xia, Y.-J.; Lin, J.; Fan, Q.-L.; Wang, L.-H.; Huang, W. *J. Phys. Chem. C* **2007**, *111*, 1166–1175. (e) Zhang, M.; Lu, P.; Wang, X.; He, L.; Xia, H.; Zhang, W.; Yang, B.; Liu, L.; Yang, L.; Yang, M.; Ma, Y.; Feng, J.; Wang, J.; Tamai, N. *J. Phys. Chem. B* **2004**, *108*, 13185–13190. (f) Chen, X.; Liao, J.-L.; Liang, Y.; Ahmed, M. O.; Tseng, H.-E.; Chen, S.-A. *J. Am. Chem. Soc.* **2003**, *125*, 636–637.

(19) Phosphorescent cyclometalated (C[∞]N) transition metal complexes derived from the building blocks described in this paper will be reported elsewhere.

(20) (a) Okamoto, I.; Ohwada, T.; Shudo, K. *J. Org. Chem.* **1996**, *61*, 3155–3166. (b) Smet, M.; Corens, D.; van Meervelt, L.; Dehaen, W. *Molecules* **2000**, *5*, 179–181.

(21) Chaturvedi, J.; Verma, S. M. *Indian J. Chem. Sect. B* **1990**, *29*, 9–13.

(22) (a) Mizzoni, R. H.; Spoerri, P. E. *J. Am. Chem. Soc.* **1951**, *73*, 1873–1874. (b) Mizzoni, R. H.; Spoerri, P. E. *J. Am. Chem. Soc.* **1954**, *76*, 2201–2203.

(23) (a) Song, Z. J.; Zhao, M.; Desmond, R.; Devine, P.; Tschaen, D. M.; Tillyer, R.; Frey, L.; Heid, R.; Xu, F.; Foster, B.; Li, J.; Reamer, R.; Volante, R.; Grabowski, E. J. J.; Dolling, U. H.; Reider, P. J.; Okada, S.; Kato, Y.; Mano, E. *J. Org. Chem.* **1999**, *64*, 9658–9667. (b) Kato, Y.; Okada, S.; Tomimoto, K.; Mase, T. *Tetrahedron Lett.* **2001**, *42*, 4849–4851.

(12) (a) Becker, H.; Ho, P. T.; Kolb, H. C.; Loren, S.; Norrby, P.-O.; Sharpless, K. B. *Tetrahedron Lett.* **1994**, *35*(40), 7315–7318. (b) Gorgues, A.; Le Coq, A. *J. Chem. Soc. Chem. Commun.* **1979**, 767–768. (c) Baumgartner, P.; Hugel, G. *Bull. Soc. Chim. Fr.* **1954**, 1005–1011.

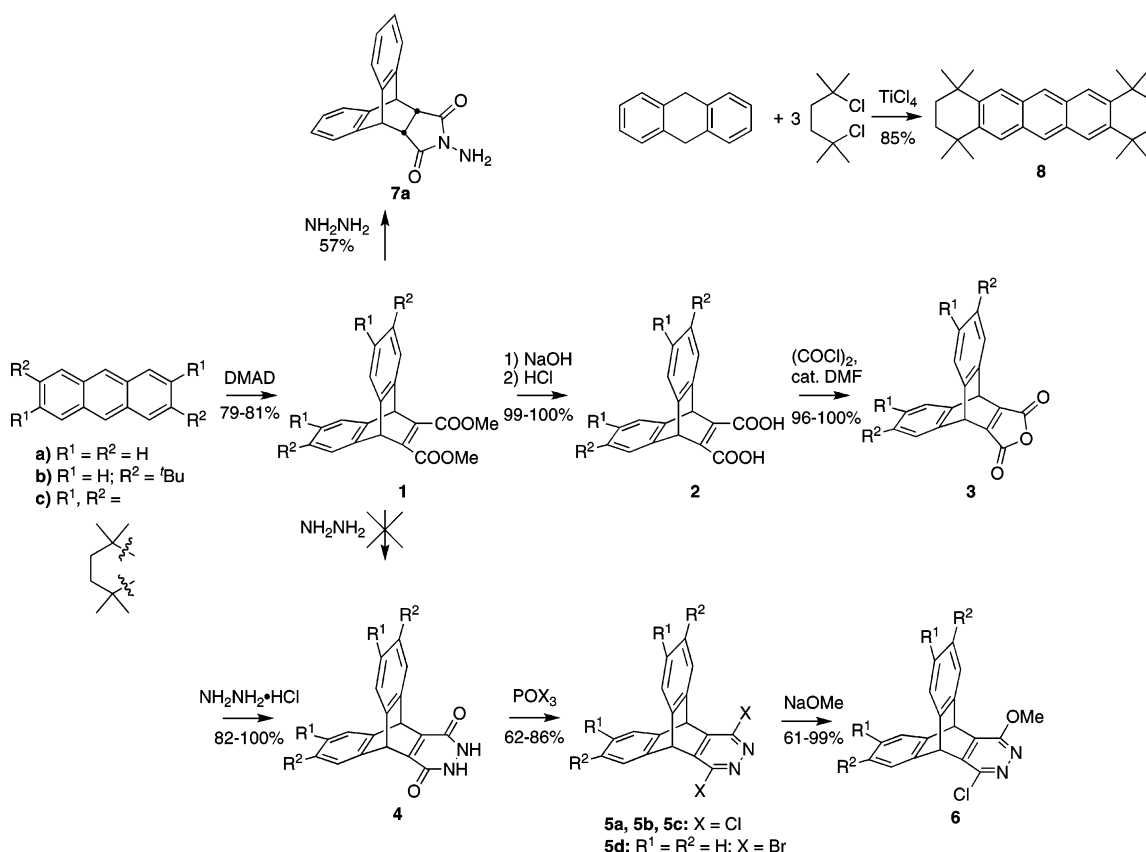
(13) (a) Kim, Y.; Swager, T. M. *Chem. Commun.* **2005**, 372–374. (b) Lux, A.; Holmes, A. B.; Cervini, R.; Davies, J. E.; Moratti, S. C.; Grüner, J.; Cacialli, F.; Friend, R. H. *Synth. Met.* **1997**, *84*, 293–294.

(14) For reviews: (a) Hughes, G.; Bryce, M. R. *J. Mater. Chem.* **2005**, *94*–107. (b) Newman, C. R.; Frisbie, C. D.; da Silva Filho, D. A.; Brédas, J.-L.; Ewbank, P. C.; Mann, K. R. *Chem. Mater.* **2004**, *16*, 4436–4451. (c) Kraft, A.; Grimsdale, A. C.; Holmes, A. B. *Angew. Chem., Int. Ed.* **1998**, *37*, 402–428. Recent examples: (d) Yoon, M.-H.; Facchetti, A.; Stern, C. E.; Marks, T. J. *J. Am. Chem. Soc.* **2006**, *128*, 5792–5801. (e) Facchetti, A.; Mushrush, M.; Yoon, M.-H.; Hutchison, G. R.; Ratner, M. A.; Marks, T. J. *J. Am. Chem. Soc.* **2004**, *126*, 13859–13874.

(15) (a) Nesterov, E. E.; Zhu, Z.; Swager, T. M. *J. Am. Chem. Soc.* **2005**, *127*, 10083–10088. (b) Zhu, Z.; Swager, T. M. *J. Am. Chem. Soc.* **2002**, *124*, 9670–9671. (c) Kim, J.; Levitsky, I. A.; McQuade, D. T.; Swager, T. M. *J. Am. Chem. Soc.* **2002**, *124*, 7710–7718. (d) Kim, J.; Swager, T. M. *Nature* **2001**, *401*, 1030–1034.

(16) (a) Cuccia, L. A.; Lehn, J.-M.; Homo, J.-C.; Schmutz, M. *Angew. Chem., Int. Ed.* **2000**, *39*, 233–237. (b) Ohkita, M.; Lehn, J.-M.; Baum, G.; Fenske, D. *Chem. Eur. J.* **1999**, *5*, 3471–3481. (c) Howard, S. T. *J. Am. Chem. Soc.* **1996**, *118*, 10269–10274. (d) Yasuda, T.; Sakai, Y.; Aramaki, S.; Yamamoto, T. *Chem. Mater.* **2005**, *17*, 6060–6068.

SCHEME 2



preparation that offered yields comparable to that of phosphorus oxybromide in the melt. Selective S_NAr reaction with sodium methoxide in tetrahydrofuran²⁴ affords the methoxy chloride **6** in excellent yield. It is worthy of note that the entire sequence of reactions up to the methoxy chloride **6** does not require chromatographic purification beyond that of a simple plug filtration, allowing for the expeditious preparation of large quantities (multigram) of these building blocks.

More soluble analogues of the pyridazine building blocks (**1–6b,c**) were obtained through the same synthetic route starting with alkylated anthracenes. Since 2,6-di-*tert*-butylantracene is not easily obtained in large quantities,²⁵ and results in racemic mixtures of the chiral intermediate iptycenes, we sought to prepare symmetrically 2,3,6,7-tetrasubstituted anthracenes bearing solubilizing alkyl groups. Only a few symmetrically 2,3,6,7-tetrasubstituted anthracenes, such as 2,3,6,7-tetramethylantracene²⁶ and 2,3,6,7-tetramethoxyanthracene,²⁷ are readily available in large quantities at a minimal synthetic or monetary cost. Given the uncertainty that these analogues would provide the desired improvement in solubility of the resulting building blocks, we optimized a double Friedel–Crafts annulation route that provides the exceptionally soluble octamethyloctahydropentacene **8** in large quantities (up to 50 g) and in excellent

yield in a single step starting from the readily available 9,10-dihydroanthracene and 2,5-dichloro-2,5-dimethylhexane (Scheme 2).

Synthesis of Iptycene-Derived Phthalazines. A synthesis of iptycene-derived phthalazines that parallels that of iptycene-derived pyridazines has been developed (Scheme 3). The Diels–Alder cycloaddition of the exocyclic diene **9a** with dimethyl acetylenedicarboxylate (DMAD),²⁸ followed by an oxidative rearomatization with potassium permanganate in the presence of a phase-transfer catalyst,²⁹ afforded the dimethyl phthalate **11a**. Unlike the corresponding dimethyl maleate **1a**, this compound reacts with hydrazine to yield the desired phthalhydrazide **12a**, which undergoes chlorination with phosphorus oxychloride to give **13a**. Subsequent treatment with sodium methoxide affords the methoxy chloride **14a**. A more soluble, alkylated analogue was prepared starting from the previously reported Diels–Alder adduct **15**.^{8c} The exocyclic diene **9b** was obtained after a series of functional group transformations and carried through the previously described synthetic route to prepare the alkylated phthalazine **13b**.

Symmetrical and Unsymmetrical Cross-Couplings. Transition metal-catalyzed cross-coupling reactions, especially with Ni^0 and Pd^0 , are the pinnacle of methodologies for the construction of conjugated materials. Consequently, we explored cross-coupling reactions with newly synthesized halopyridazines (**5a–d**, **6a–c**) to generate symmetrically or unsymmetrically 3,6-disubstituted iptycene-derived pyridazines (Scheme 4 and Table 1). The pyridazine ring was found to be sufficiently

(24) Lee, J. I.; Park, H.; Yun, Y. S.; Kwon, S. K. *J. Korean Chem. Soc.* **2001**, *45*, 386–390.

(25) See the Supporting Information for discussion.

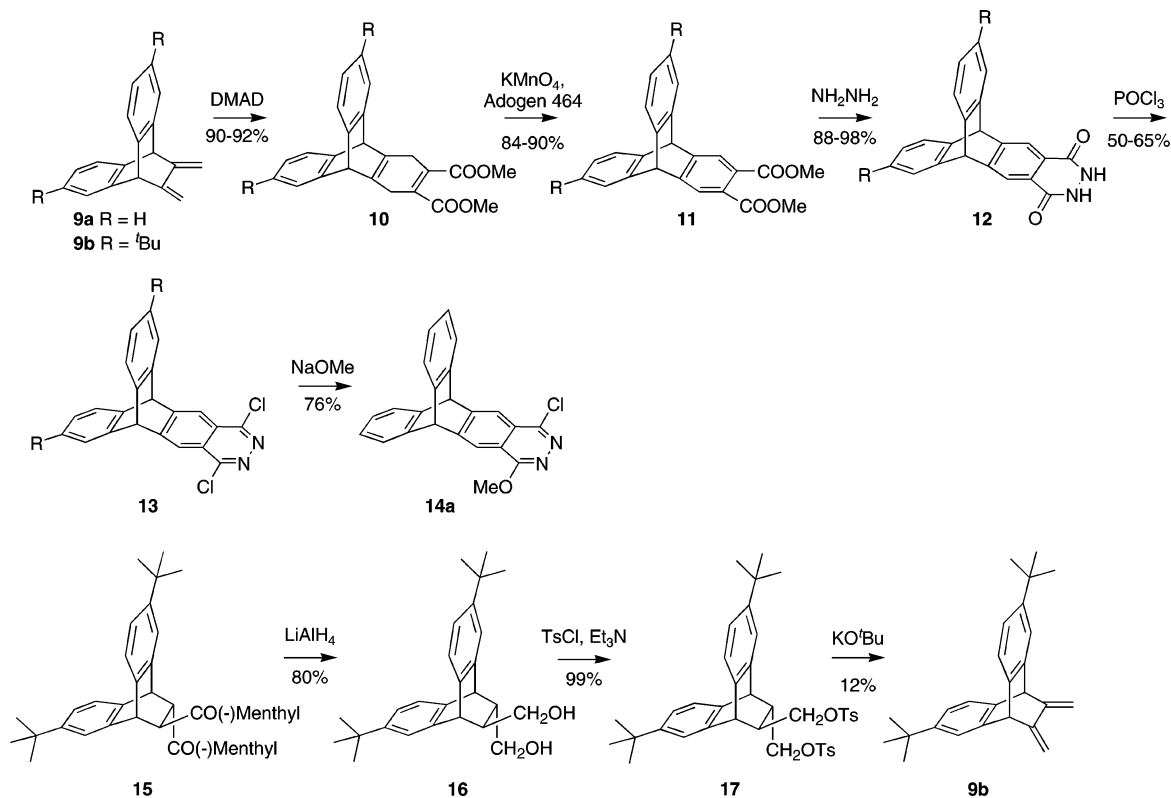
(26) (a) Hinshaw, J. C. *Org. Prep. Proced. Int.* **1972**, *4*, 211–213. (b) Godinez, C. E.; Zepeda, G.; Mortko, C. J.; Dang, H.; Garcia-Garibay, M. A. *J. Org. Chem.* **2004**, *69*, 1652–1662.

(27) (a) Robinson, G. M. *J. Chem. Soc. Trans.* **1915**, *107*, 267–276. (b) Miao, Q.; Nguyen, T.-Q.; Someya, T.; Blanchet, G. B.; Nuckolls, C. J. *Am. Chem. Soc.* **2003**, *125*, 10284–10287.

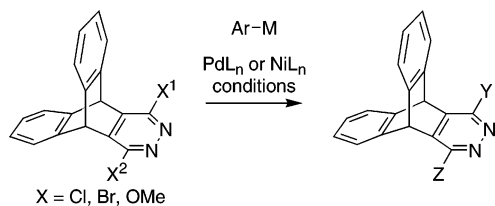
(28) Butler, D. N.; Snow, R. A. *Can. J. Chem.* **1975**, *53*, 256–262.

(29) Poulou, A.; Croteau, R. *J. Chem. Soc., Chem. Commun.* **1979**, 243–244.

SCHEME 3



SCHEME 4



electron deficient and activated for oxidative addition with standard palladium catalysts even for the nominally less reactive chlorides. Concomitantly, the high degree of electronic activation of the chloropyridazines accelerates nucleophilic aromatic substitution by nucleophiles such as amines, hydroxide, or alkoxides. These side reactions prevent Suzuki–Miyaura cross-coupling reactions of the chloropyridazines under typical biphasic reactions conditions (e.g., toluene-aqueous base) without significant competing hydrolysis. The Suzuki–Miyaura couplings proceed smoothly, however, in anhydrous dioxane in the presence of cesium fluoride as a base. These reaction conditions also appear optimal for Stille cross-coupling reactions. A nickel-catalyzed Negishi cross-coupling reaction was also adequate for the preparation of the 3,6-bis(bithienyl) derivative **20** in yields comparable to those obtained with the corresponding Stille reaction. Improved reactivity with increased electron-rich character of the nucleophilic cross-coupling partner was observed in most cases. Thus, forcing conditions³⁰ are required for the reaction between the chloromethoxy pyridazine **6a** and 2,4-difluorobenzeneboronic acid, and the desired cross-

(30) Korenaga, T.; Kosaki, T.; Fukumura, R.; Ema, T.; Sakai, T. *Org. Lett.* **2005**, *7*, 4916–4917.

coupling product **23** is only obtained in poor yield. We also observe a counter-statistical bias during cross-coupling of the dichloride **5a** with <1 equiv of the organometallic reagent, which precludes the clean formation of the mono-cross-coupled products (e.g., **25**). Therefore, it was found to be preferable to perform the cross-coupling of the chloromethoxy pyridazine **6a**, and to subsequently convert the intermediate **22** to the corresponding chloropyridazine (Scheme 5). Alternately, if one requires a monosubstituted pyridazine, hydrodechlorination of the chloromethoxy pyridazine **6a** followed by deprotection and chlorination yields the chloropyridazine **30**.

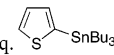
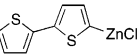
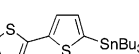
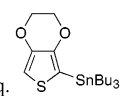
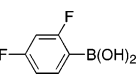
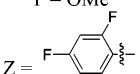
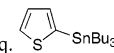
Reductive Dimerizations. We have explored chemistries that would allow dimerization, and ultimately polymerization of the novel iptycene-derived diazines.³¹ Having demonstrated that the chloro and bromo diazines are good *electrophilic* partners in cross-coupling reactions, we sought to prepare the corresponding *nucleophilic* cross-coupling partners. Many attempts for the preparation of iptycene-derived pyridazines metalated at the 3- and/or the 6-position to yield the corresponding Kumada, Negishi, Stille, or Suzuki–Miyaura reagents were unsuccessful. Attempts to homopolymerize the dihalopyridazines **5a–d** with bis(boronates)³² or bis(stannanes)^{16d,33} were similarly unsuccessful. These limitations are likely the result of the known instability and/or susceptibility to protodemetalation of metalated

(31) Polymers incorporating iptycene-derived pyridazines will be reported elsewhere.

(32) Rabindranath, A. R.; Zhu, Y.; Heim, I.; Tieke, B. *Macromolecules* **2006**, *39*, 8250–8256.

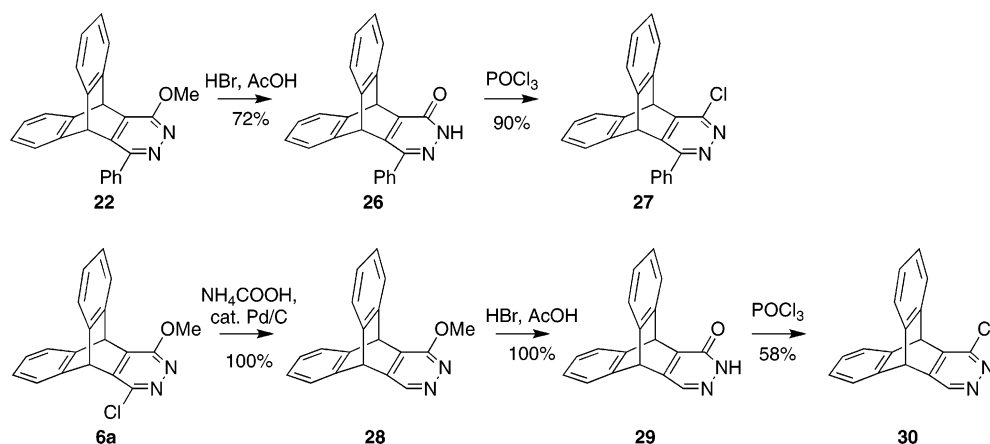
(33) (a) Nielsen, C. B.; Bjørnholm, T. *Org. Lett.* **2004**, *6*, 3381–3384. (b) Zhu, Y.; Champion, R. D.; Jenekhe, S. A. *Macromolecules* **2006**, *39*, 8712–8719. (c) Devasagayaraj, A.; Tour, J. M. *Macromolecules* **1999**, *32*, 6425–6430. (d) Xu, J.; Ng, S. C.; Chan, H. S. O. *Tetrahedron Lett.* **2001**, *42*, 5327–5329.

TABLE 1. Cross-Coupling Reactions

X ¹ , X ²	Ar-M	Conditions ^a	Product
X ¹ = X ² = Cl (5a)	3 eq. PhSnMe ₃	A	Y = Z = Ph (18) (54%)
X ¹ = X ² = Cl (5a)	3 eq. PhB(OH) ₂	B	Y = Z = Ph (18) (83%)
X ¹ = X ² = Cl (5a)	3 eq. 	A	Y = Z = 2-thienyl (19) (95%)
X ¹ = X ² = Cl (5a)	4 eq. 	C	Y = Z = 2,2'-bithiophen-5-yl (20) (77%)
X ¹ = X ² = Cl (5a)	4 eq. 	A	Y = Z = 2,2'-bithiophen-5-yl (20) (86%)
X ¹ = X ² = Cl (5a)	4 eq. 	A	Y = Z = 3,4-ethylenedioxythiophen-2-yl (21) (85%)
X ¹ = OMe; X ² = Cl (6a)	1.8 eq. PhB(OH) ₂	A	Y = OMe; Z = Ph (22) (91%)
X ¹ = OMe; X ² = Cl (6a)	2 eq. 	D	Y = OMe Z =  (23) (37%)
X ¹ = H; X ² = Cl (30)	2 eq. PhB(OH) ₂	A	Y = H; Z = Ph (24) (64%)
X ¹ = H; X ² = Cl (30)	2 eq. 	A	Y = H; Z = 2-thienyl (25) (78%)

^a Conditions (see the Supporting Information for details): (A) 5% Pd(PPh₃)₄, CsF, *p*-dioxane, 100–110 °C; (B) 1.5% Pd₂(dba)₃, 6% ^tBu₃P·HBF₄, CsF, *p*-dioxane, 100–110 °C; (C) 5% Ni(dppp)Cl₂, THF, 60 °C; (D) 5% Pd₂(dba)₃, 12% ^tBu₃P·HBF₄, CsF, Ag₂O, DMF, 100 °C.

SCHEME 5



electron-poor nitrogen heterocycles.³⁴ In fact, although 3-halopyridazines are commonly employed as electrophilic partners in cross-coupling reactions, we are only aware of two reports where pyridazines metalated in the 3-position are used as

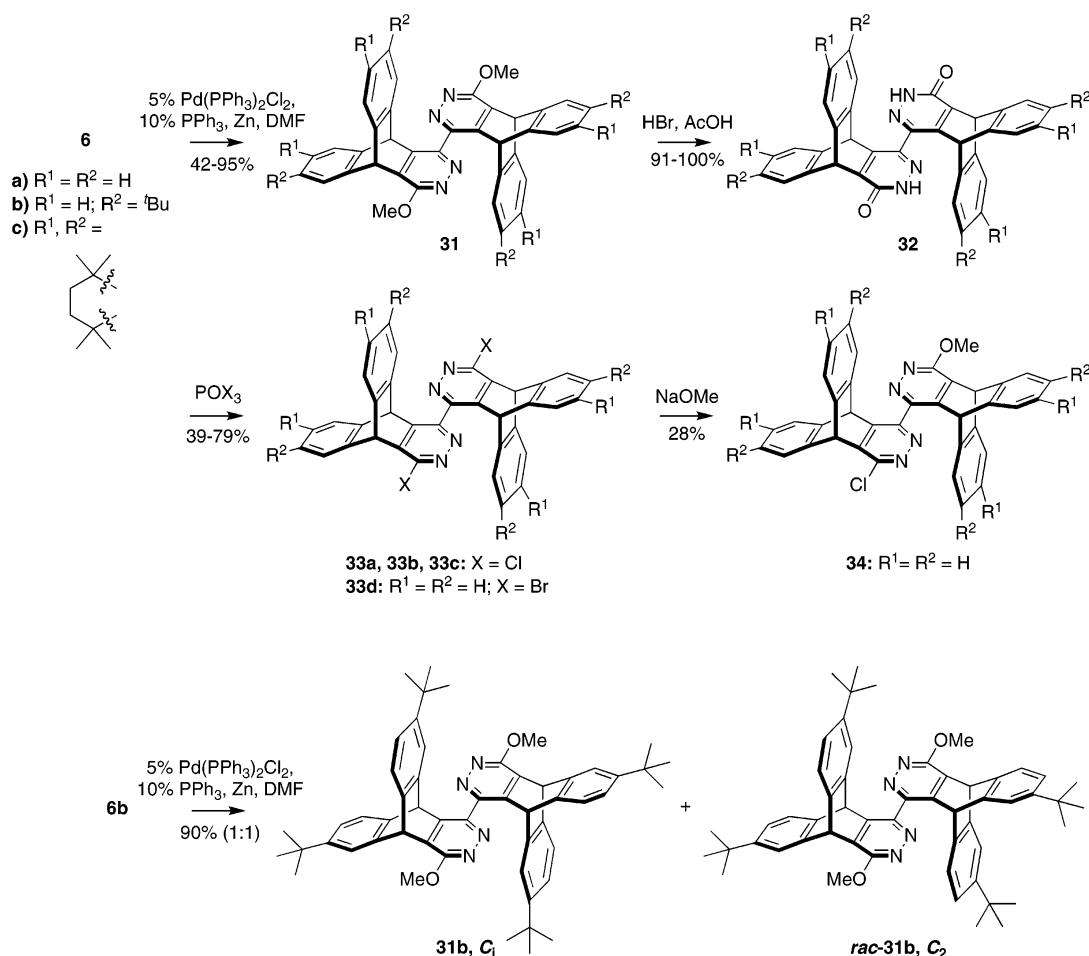
nucleophilic partners in standard cross-coupling reactions.³⁵ Furthermore, to address the difficulties associated with electron-deficient heterocyclic couplings, alternate methods based on the direct arylation of pyridazine *N*-oxides with aryl halides through C–H bond activation have been developed.³⁶ Nevertheless, we considered these alternate methodologies to be ill-suited for our

(34) (a) Matondo, H.; Souirti, S.; Baboulène, M. *Synth. Commun.* **2003**, *33*, 795–800. (b) Gros, P.; Doudouh, A.; Fort, Y. *Tetrahedron Lett.* **2004**, *45*, 6239–6241. (c) Hodgson, P. B.; Salingue, F. H. *Tetrahedron Lett.* **2004**, *45*, 685–687. (d) Darabantu, M.; Bouilly, L.; Turck, A.; Plé, N. *Tetrahedron* **2005**, *61*, 2897–2905. (e) Bouillon, A.; Lancelot, J.-C.; de Oliveira Santos, J. S.; Collot, V.; Bovy, P. R.; Rault, S. *Tetrahedron* **2003**, *59*, 10043–10049. (f) Ishiyama, T.; Ishida, K.; Miyaura, N. *Tetrahedron* **2000**, *57*, 9813–9816. (g) Fischer, F. C.; Havinga, E. *Recl. Trav. Chim. Pays-Bas* **1974**, *93*, 21–24. (h) Gilman, H.; Spatz, S. M. *J. Org. Chem.* **1951**, *16*, 1485–1494.

(35) (a) Boger, D. L.; Miyauchi, H.; Du, W.; Hardouin, C.; Fecik, R. A.; Cheng, H.; Hwang, I.; Hedrick, M. P.; Leung, D.; Acevedo, O.; Guimaraes, C. R. W.; Jorgensen, W. L.; Cravatt, B. F. *J. Med. Chem.* **2005**, *48*, 1849–1856. (b) Imin, P.; Imit, M.; Jamal, R.; Nurulla, I. *Gongneng Gaofenzi Xuebao (J. Funct. Polym.)* **2005**, *18*, 290–294.

(36) (a) Campeau, L.-C.; Rousseaux, S.; Fagnou, K. *J. Am. Chem. Soc.* **2005**, *127*, 18020–18021. (b) Leclerc, J.-P.; Fagnou, K. *Angew. Chem., Ind. Ed.* **2006**, *45*, 7781–7786.

SCHEME 6



targets. Inspired by reports of nickel- and palladium-mediated reductive homocoupling of chloropyridazines,³⁷ the reductive homopolymerization of the dihalopyridazines **5a–d** was explored. Reductive homopolymerization attempts under Yamamoto conditions ($Ni(cod)_2$, *bpy*)³⁸ did not yield the desired homopolymers and dehalogenated low molecular weight materials were the dominant products. Various attempts directed at the improvement of this reaction by varying the transition metal (pre)-catalyst³⁹ and stoichiometric reductant⁴⁰ were similarly unsuccessful.

Prompted by the observations that electron-poor arenes or heteroarenes were poor nucleophilic partners in cross-coupling reactions with the halopyridazines (vide supra), and that oxidative addition to the halopyridazine electrophilic partner did not appear to be limiting, the dimerization of the 3-chloropyridazines **6a–c** bearing an electron-donating methoxy group at the para position was explored. Homocoupling of **6a**

following the protocol described by Lehn and Baxter,^{37a} using 30% $NiBr_2(PPh_3)_3$, tBu_4NI , and zinc dust in *N,N'*-dimethylformamide, afforded only 11% of dimer **31a**. Addition of 2,2'-bipyridine as a ligand and increasing the catalyst loading to 300 mol % resulted in a moderate yield (60–65%) of the dimer **31a**, with significant quantities of the hydrodehalogenated methoxypyridazine **28** as a byproduct. These observations suggest that catalytic turnover is very limited in this system. However, it was found that the use of catalytic amounts of a palladium precatalyst with zinc dust as the stoichiometric reductant⁴¹ enabled the reductive homocoupling to efficiently afford the dimer **31a**. Further optimization of the reaction conditions (5% $Pd(PPh_3)_2Cl_2$, 10% PPh_3 , Zn, DMF, 100 °C) enabled the homocoupling to proceed reliably and cleanly in excellent yields (93–95%). Interestingly, after screening a variety of ligands and precatalysts for this transformation, we found the use of either $Pd(PPh_3)_2Cl_2/PPh_3$ or $Pd(PPh_3)_4$ to be optimal, and the use of advanced catalytic systems (e.g., bulky trialkylphosphines, biaryldialkylphosphines, NHCs, etc.) did not result in an improvement of the reaction.

Since the alkylated methoxy chloride **6b** has been prepared as an unresolved mixture of enantiomers, the reductive homocoupling resulted in the diastereoisomeric dimethoxy dimers

(37) (a) Baxter, P. N. W.; Lehn, J.-M.; Baum, G.; Fenske, D. *Chem. Eur. J.* **2000**, *6* (24), 4510–4517. (b) Bouilly, L.; Darabantu, M.; Turck, A.; Plé, N. *J. Heterocycl. Chem.* **2005**, *42*, 1423–1428.

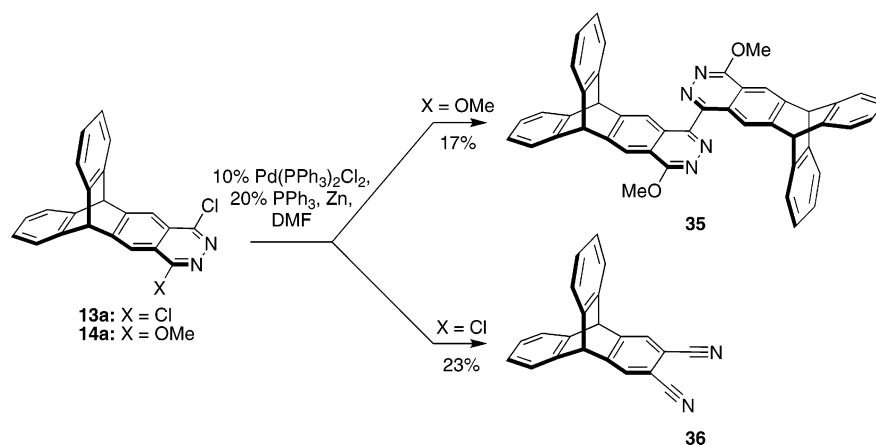
(38) (a) Yamamoto, T.; Morita, A.; Miyazaki, Y.; Maruyama, T.; Wakayama, H.; Zhou, Z.-h.; Nakamura, Y.; Kanbara, T.; Sasaki, S.; Kubota, K. *Macromolecules* **1992**, *25*, 1214–1223. (b) Yamamoto, T.; Maruyama, T.; Zhou, Z.-h.; Ito, T.; Fukuda, T.; Yoneda, Y.; Begum, F.; Ikeda, T.; Sasaki, S.; Takezoe, H.; Fukuda, A.; Kubota, K. *J. Am. Chem. Soc.* **1994**, *116*, 4832–4845.

(39) Ni, Pd, and Cu pre-catalysts, various combinations of transition metal salt/complexes, and ligands were screened.

(40) Zn^0 , Mg^0 , Al^0 , In^0 , Ni^0 complexes, Mn^0 , Sn^0 , hydroquinones, and 1,1,2,2-tetra(pyrrolidin-1-yl)ethene (a TDAE analogue) were screened.

(41) (a) Lee, T.-S.; An, J. H.; Kim, J.; Bae, J.-Y. *Bull. Korean Chem. Soc.* **2001**, *22*, 375–378. (b) Jutand, A.; Mosleh, A. *Synlett* **1993**, *8*, 568–570. (c) Amatore, C.; Carré, E.; Jutand, A.; Tanaka, H.; Ren, Q.; Torii, S. *Chem. Eur. J.* **1996**, *2*, 957–966. (d) Jutand, A.; Mosleh, A. *J. Org. Chem.* **1997**, *62*, 261–274.

SCHEME 7



31b, *C_i*, and *rac*-**31b**, *C₂* (Scheme 6). The isomers are obtained in a 1:1 ratio, and may be separated by column chromatography. Despite their remarkably similar structures, the diastereomers exhibit distinct spectroscopic features. The ¹H NMR spectra of the mixture of diastereomers shows the four distinct, well-resolved resonances of each of the chemically nonequivalent *tert*-butyl groups, the two distinct resonances of the methoxy groups, and although the signals of the two “external” bridgehead protons overlap, the pair of “internal” bridgehead proton signals are spaced more than 0.2 ppm apart. Attempts at obtaining X-ray quality single crystals of either isomer of **31b**, **32b**, and **33b** were unsuccessful. Moreover, while COSY and NOE ¹H NMR experiments gave self-consistent results, it has been impossible to unequivocally assign the structure of each isomer. Reductive coupling of the alkylated methoxy chloride **6c** gave the symmetrically alkylated dimer **31c**. The isolation and purification of **31c** were hindered by its limited solubility in most organic solvents with the exception of hot toluene, carbon disulfide, and heavier chlorinated solvents (e.g., tri- and tetrachloroethylene, tetrachloroethane). It is surprising that, while the symmetrically alkylated anthracene **8** and monomeric intermediates **1c**–**6c** are considerably *more* soluble in typical organic solvents than either of their parent compounds **1a**–**6a** or *tert*-butyl-substituted **1b**–**6b** counterparts, the dimers **31c**, **32c**, and **33c** are markedly *less* soluble than their parent compounds **31a**–**33a** or *tert*-butyl-substituted counterparts **31b**–**33b**.

The dimethoxy dimers **31a**–**c** could be converted to the corresponding dihalides by cleavage of the methoxy groups with hydrobromic acid in acetic acid, followed by treatment with a phosphorus(V) oxyhalide to give the dihalo dimers **33a**–**d** in moderate to good yields. Treatment of the dichloride **33a** with sodium methoxide in THF afforded the chloro methoxy dimer **34** in low yield (28%, 47% based on recovered starting material). The nucleophilic substitution of **5a**–**c** to **6a**–**c** is selective for the monomethoxy product due to the deactivating effect of the first methoxy group for further ring substitution. By contrast, the conversion from **33a** to **34** shows little selectivity, and consequently, a mixture of the starting dichloro dimer **33a**, the chloro methoxy dimer **34**, and the dimethoxy dimer **31a** is obtained.

The reductive coupling of dichlorophthalazine **13a** and chloromethoxyphthalazine **14a** was similarly explored (Scheme 7). In parallel with what was observed with the corresponding pyridazines (**5a**–**c**, **6a**–**c**), the dichlorophthalazine **13a** did not participate in reductive homopolymerization under the reaction

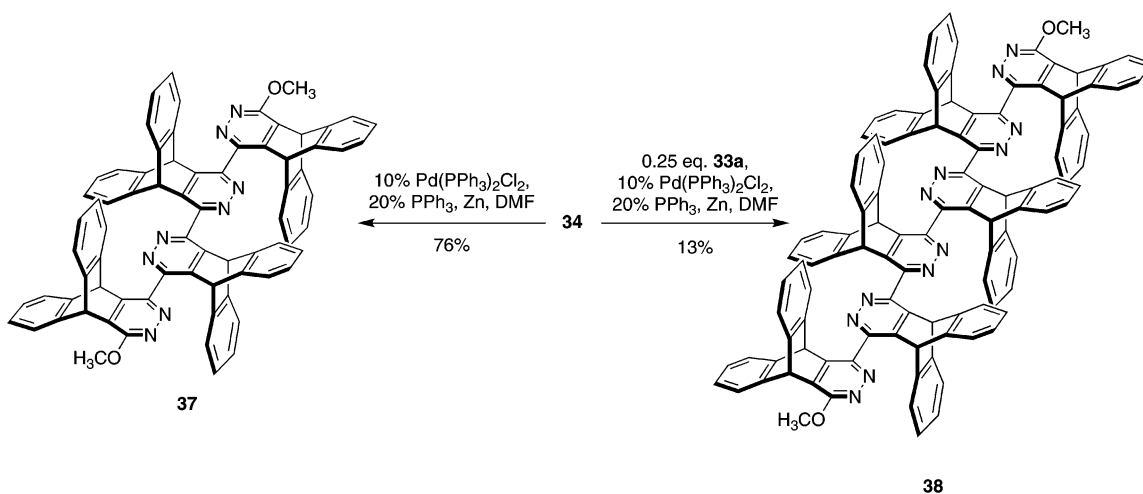
conditions surveyed. The reductive dimerization of the chloromethoxyphthalazine **14a** was best accomplished with zinc dust in *N,N*-dimethylformamide in the presence of a catalytic amount of a palladium precatalyst. The isolated yields of the dimethoxybiphthalazine **35** were poor (17%) in comparison to the analogous reaction carried out with the chloromethoxyphthalazine **6a** (up to 95%). Furthermore, under these reaction conditions the reaction mixture rapidly displayed a deep purple hue, which disappeared upon aqueous workup. By contrast, no coloration develops in the reductive dimerization of the pyridazines **6a**–**c**. This intriguing difference in the chemical behavior of otherwise similarly behaved species is highlighted by the isolation of 2,3-dicyanotriptycene (**36**)⁴² in 23% yield from the reaction mixture when **13a** is used as a starting material.

The transformation of a chlorophthalazine into a 1,2-dicyanobenzene is not unprecedented. Yanilkin and co-workers⁴³ have reported that both the chemical reduction with metallic potassium and the electrochemical reduction of 1-chloro-4-*X*-phthalazines (X = Cl, OPh, OMe, OEt, OⁱPr) in *N,N*-dimethylformamide yield the radical anion of phthalonitrile. The situation observed with the chlorophthalazines **13a** and **14a** appears slightly more complex. While treatment of **13a** with zinc dust in DMF in the absence of a palladium catalyst affords 2,3-dicyanotriptycene **36**, the reaction is much slower than in the presence of 0.1 equiv of Pd(PPh₃)₂Cl₂ and 0.2 equiv of PPh₃. In the latter case, the deep blue-purple hue attributed to the radical anion of 2,3-dicyanotriptycene **36** appears within 2 h at 60 °C. By contrast, in the absence of a palladium catalyst, the color only arises after several hours at 120 °C. The reaction with the more electron rich chloromethoxyphthalazine **14a** is markedly slower. In the absence of a palladium catalyst, **14a** is only slowly degraded with zinc dust in DMF at 120 °C, and 2,3-dicyanotriptycene **36** and the protodehalogenated 1-methoxyphthalazine are the only identifiable trace byproducts (3% and 5%, respectively). Finally, the reaction of **14a** with zinc dust in DMF in the presence of a palladium catalyst (0.1 equiv of Pd(PPh₃)₂Cl₂ and 0.2 equiv of PPh₃) requires a reaction temperature higher than that for **13a** (100 °C) to yield dimethoxy dimer **35** as the sole identifiable product by ¹H NMR. The deep-

(42) (a) Gal'pern, M. A.; Shalaev, V. K.; Shatsskaya, T. A.; Shishkanova, L. S.; Skvarchenko, V. R.; Luk'yanets, E. A. *Zh. Obshch. Khim.* **1983**, *53*, 2601–2606. (b) Shatsskaya, T. A.; Gal'pern, M. G.; Skvarchenko, V. R.; Luk'yanets, E. A. *Vest. Moskov. Univ. Khim.* **1986**, *41*, 64–66.

(43) Yankilin, V. V.; Buzykin, B. I.; Morozov, V. I.; Nastapova, N. V.; Maksimyyuk, N. I.; Eliseenkova, R. M. *Zh. Obshch. Khim.* **2001**, *71*, 1726–1737.

SCHEME 8



purple color of the reaction mixture suggests that traces of 2,3-dicyanotriptycene **36** are nonetheless generated. These constitute evidence for the involvement of the palladium catalyst in the reductive heterocyclic ring-opening reactions, though the exact nature of this involvement has not been elucidated. These competing side reactions were directly observed with the iptycene-derived phthalazines (**13a**, **14a**), but not with the analogous pyridazines (**5a–c**, **6a–c**), possibly because they might show a more negative reduction potential. One is tempted to speculate that, were such competing pathways to occur, they might, along with protodehalogenation, be significant limitations to the synthesis of homopolymers of **5a–d** through reductive coupling routes (vide supra).

Higher Oligopyridazines Through Controlled Approaches.

Optimized reductive coupling conditions were applied to the preparation of extended oligopyridazines (Scheme 8). Under these conditions, the reductive coupling of the chloro methoxy dimer **34** proceeds smoothly in good yield (76%) to afford the quaterpyridazine **37**. Unlike previously reported quaterpyridazines, which showed poor solubility,^{37a} the tetramer **37** is freely soluble in a variety of common organic solvents, such as chloroform, dichloromethane, toluene, ethyl acetate, tetrahydrofuran, and acetone. The comparatively high solubility of **37** is attributed to the iptycene scaffold, which prevents the strong π - π stacking interactions in the solid state that impede dissolution. When an excess (4 equiv) of the chloro methoxy dimer **34** is reductively coupled in the presence of the dichloro dimer **33a**, the tetramer **37** (24%) and small quantities of the hexamer (**38**) (~10–15%) can be obtained after chromatographic separation. This hexamer represents, to the best of our knowledge, the first example of a fully characterized sexipyridazine. Interestingly, the solubility of the hexamer **38** is qualitatively comparable to that of tetramer **37**.

Planarity and Conjugation of Biaryls Obtained from Iptycene-Derived Pyridazines and Phthalazines. We have used this small library of compounds containing iptycene-derived pyridazines and phthalazines to test our hypothesis that coplanarity of the biaryl linkages will be the preferred conformation. The vast majority of the compounds herein described are crystalline, and as a result a number of structures were determined by X-ray crystallography. NMR spectroscopy and computational studies also provide additional insight into the conformations of these molecules. We expected that a fully coplanar conformation about the biaryl linkage at the 3-position

of the pyridazine or phthalazine would be at least accessible, if not energetically favored through increased conjugation, for pyridazines and phthalazines attached to five-membered-ring heterarenes and six-membered-ring heterarenes bearing no ortho substituents (e.g., 2-thienyl, 3-pyridazinyl, etc.). Furthermore, we postulated that a secondary hydrogen-bonding interaction between the heteroatom of a heteraryl group and the bridgehead hydrogen of the iptycene framework might provide an additional enthalpic stabilization term.

(a) X-ray Crystallography. We examined the structure of several of the iptycene-derived diazine building blocks by X-ray crystallography to ascertain the validity of the coplanarization hypotheses. In conducting this analysis it is important to bear in mind that intermolecular interactions and close-packing can affect the conformation of molecules in the solid state such that they are not necessarily representative of their “free” (or solvated) preferred conformations. The structures obtained for seven compounds are presented in Figure 1. The 2-thienyl derivative **19** adopts a quasicoplanar conformation of the teraryl fragment, as predicted (N–C–C–S dihedral angles: 5.05(15)° and 8.4(2)°). Interestingly, a cisoid, synperiplanar (N–C–C–S) rotamer is observed, as opposed to the predicted transoid, antiperiplanar rotamer, illustrating at once the negligible steric clash between the bridgehead hydrogen of the iptycene and the adjacent hydrogen on the 5-membered ring, and the absence of involvement of a stabilizing S–H hydrogen-bonding interaction.⁴⁴ Furthermore, within the crystal structure of **19** is also present another rotamer where the teraryl fragment is not planar but oblique (N–C–C–S dihedral angles: 29.84(16)° and 120.30(19)°), as is observed for the bis(3,4-ethylenedioxy)-thiophene-2-yl derivative **21** (N–C–C–S dihedral angles: 33.79(16)° and 37.54(15)°). These observations suggest that the 2-thienyl group can freely, or with a minimal energy barrier, rotate about the biaryl linkage. In contrast, and as expected, a phenyl substituent, as in the 2,4-difluorophenyl derivative **23**, does not adopt a coplanar conformation about the biaryl linkage (N–C–C–C_(F) dihedral angle 127.56(10)°).

The pyridazine and phthalazine dimers **31a**, **33a**, and **35** do not adopt a coplanar conformation about the biaryl linkages, despite the predicted stabilization through increased conjugation

(44) Stabilizing S–N interactions that favor a synperiplanar (cisoid) rotamer have been proposed in related compounds. See ref 16d and references therein.

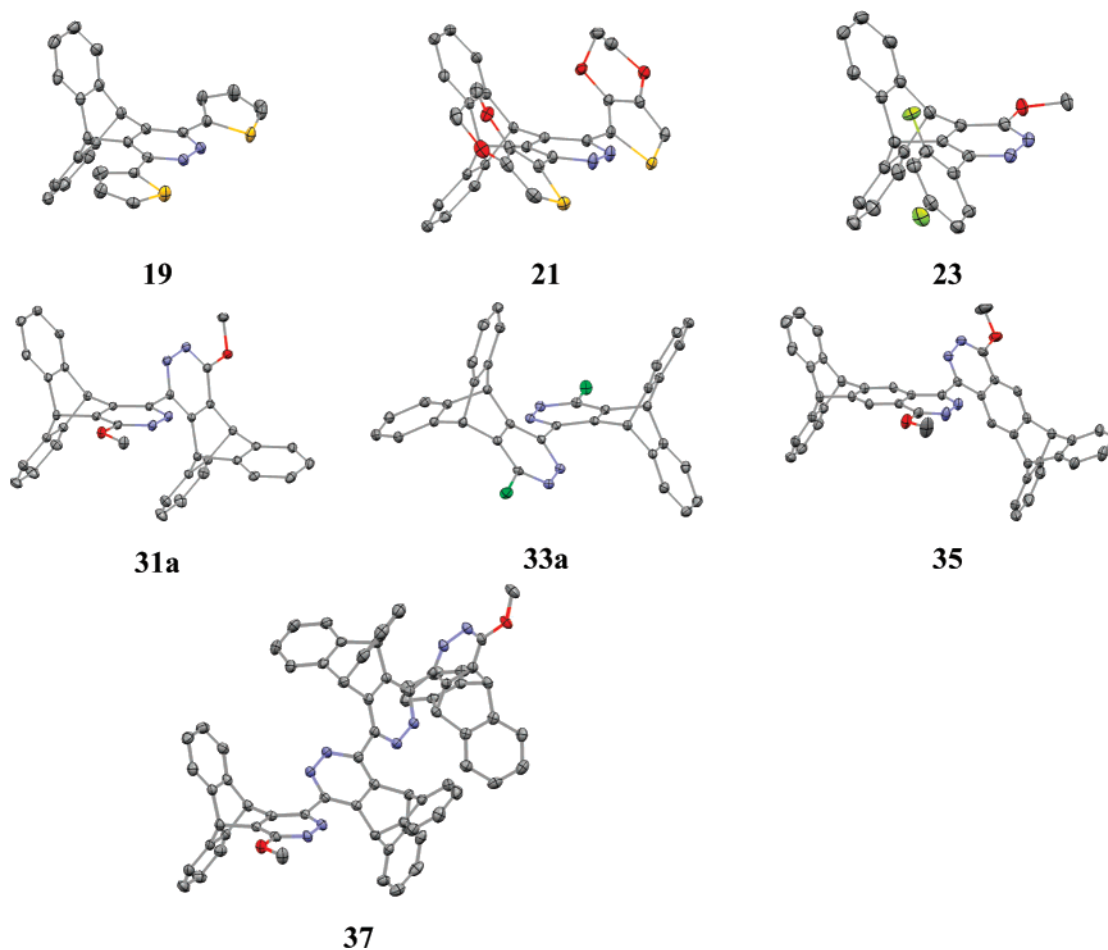


FIGURE 1. X-ray crystal structures of iptycene-derived pyridazines and phthalazines. Fifty percent probability thermal ellipsoids. Hydrogens and solvent molecules were omitted for clarity. See the Supporting Information for details.

and the possibility of weak N–H intramolecular hydrogen bonding. The inclination of the diazine rings with respect to another varies greatly in this series, from the dimethoxy dimer **31a** (N–C–C–N dihedral angle $113.70(13)^\circ$) to the dichloro dimer **33a** (N–C–C–N dihedral angle $135.07(15)^\circ$), with an intermediate value for the phthalazine dimer **35** (N–C–C–N dihedral angle $127.4(2)^\circ$). For the former pair of compounds, it is unlikely that the steric and electronic parameters are affected by the substitution of a methoxy group for a chlorine atom at a position remote to the biaryl linkage. These results suggest that, at least within this bracket of torsion angles, the potential energy curve for rotation about the biaryl linkage must be shallow enough that intermolecular interactions and close packing overcome an inherently preferred rotamer. Finally, the structure of the tetramer **37** reveals that a further extension of the conjugation might favor coplanarization of the oligoheteraryl segments, even though an overall loss of linearity of the structure due to bending is witnessed (N–C–C–N dihedral angles $141.58(17)^\circ$, $141.07(17)^\circ$, $141.51(16)^\circ$). It should finally be stressed that X-ray crystallography provided no evidence of intramolecular hydrogen bonding between the iptycene and a proximal heteroatom in any of the structures herein described.

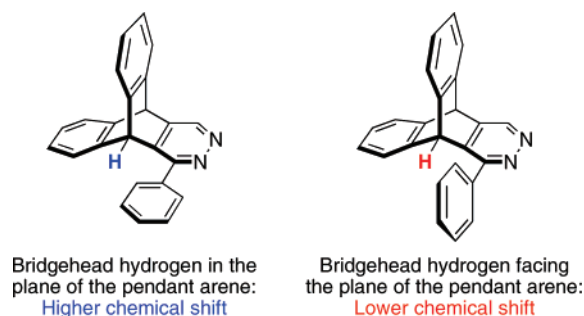
(b) NMR Spectroscopy. The ^1H NMR resonance of the bridgehead hydrogen of triptycene appears at 5.41 ppm in CDCl_3 . This value is unusually high for a sp^3 -hybridized hydrocarbon, as expected due to the inductive effects and ring current anisotropy of the three aromatic rings of the triptycene

molecule. This peak is not split by any adjacent nucleus, and is in a region that is free of other signals, hence it is a key diagnostic in NMR identification of compounds. We sought to take advantage of local ring current anisotropy to provide an indirect way of evaluating the coplanarity of the iptycene-derived pyridazine and phthalazine structures in solution. For a simple arylated iptycene-derived pyridazine (e.g., **18**), were the aryl groups to be completely coplanar with the pyridazine ring, one would expect the bridgehead hydrogen to experience the influence of ring current anisotropy induced by the three arenes of the iptycene-derived pyridazine scaffold, in addition to that induced by the pendant aryl group. The resulting NMR signal would be shifted downfield, in a situation reminiscent of the “bay” protons in phenanthrene and other fused polycyclic aromatic hydrocarbons. Conversely, if the pendant aryl group lies predominantly perpendicular to the plane of the pyridazine ring, the bridgehead hydrogen signal should shift upfield (Scheme 9).

In the monomeric iptycene-derived pyridazines bearing non-carbon substituents at the 3,6-positions (**5a–d**, **6a–c**, **28**, **30**), the observed chemical shift⁴⁵ of the proximal bridgehead hydrogen is within a narrow range (δ 5.61–5.85 ppm). This range is even narrower (δ 5.72–5.85 ppm) if the outlying signals

(45) All chemical shift comparisons refer to the spectra taken in CDCl_3 , referenced to the solvent resonance and expressed in ppm vs tetramethylsilane.

SCHEME 9



corresponding to the sterically congested **5c**, **6c** (δ 5.61–5.69 ppm), and the pyridazines unsubstituted at the 6-position, such as in **28** and **30** (δ 5.56–5.60 ppm), are excluded. The fact that the chemical shift of the bridgehead hydrogen in iptycene-derived pyridazines is \sim 0.2–0.4 ppm higher than that of simple triptycenes likely reflects the electron-deficient nature of the pyridazine ring. Unsymmetrically 1,4-disubstituted iptycene-derived pyridazines (**6a–c**, **22–30**) show two singlets corresponding to each of the bridgehead hydrogens, but the chemical shift difference between the two can be minimal, as observed for the bridgehead hydrogens proximal to the chloro and the methoxy substituents in **6a** ($\Delta\delta \leq 0.03$ ppm).

Substitution by a phenyl group (**18**, **22**, **24**, **27**) results only in a minimal shift of the signal assigned to the bridgehead hydrogen proximal to the phenyl substituent⁴⁶ relative to those next to a halogen or a methoxy group ($\Delta\delta -0.08$ to $+0.08$ ppm). This suggests either that the influence of the additional ring current anisotropy does not affect the proximal bridgehead hydrogen, or that the average influence of the rotamer population distribution within the NMR time scale gives no change in the chemical shift of phenyl-substituted iptycene-derived pyridazines. The latter is plausible considering that a phenyl ring will likely prefer to be oblique or gauche with respect to the plane of the pyridazine ring to avoid the eclipsing of the ortho hydrogens by the proximal bridgehead hydrogen. Substitution by a 3,4-ethylenedioxythiophen-2-yl group (**21**) has a similar effect (e.g., **5a** \rightarrow **21** $\Delta\delta = +0.12$ ppm). This is in agreement with the solid-state structure in which the substituent group is synclinal with respect to the plane of the pyridazine ring (N–C–C–S dihedral angle $\sim 35^\circ$).

Substitution by the 2,4-difluorophenyl group (**23**) results in a more significant upfield shift of the proximal bridgehead hydrogen (e.g., **6a** \rightarrow **23** $\Delta\delta = -0.36$ to 5.43 ppm). This is the lowest chemical shift observed for bridgehead hydrogens among all of the iptycene-derived pyridazines herein reported. A coplanar conformation of the pendant arene and the pyridazine ring in **23** would be energetically demanding due to the steric clash between the ortho fluorine and the proximal bridgehead hydrogen for the antiperiplanar (N–C–C–C_(F)) rotamer, and due to electronic and dipole–dipole repulsion for the synperiplanar rotamer. Among the compounds studied, the fluorinated derivative **23** is the most likely to show a predominantly perpendicular orientation between the pendant arene ring and the pyridazine ring (vide infra). A real, although weak, NOE signal enhancement (1.0%) of the ortho proton of the difluorophenyl ring upon irradiation of the proximal bridgehead

(46) This assignment is confirmed by a NOE enhancement of the ortho proton of the phenyl ring (+6.0–7.3%) upon irradiation of the proximal bridgehead hydrogen. See the Supporting Information for details.

hydrogen supports both the assignment of the proximal bridgehead hydrogen and a preferred or time-averaged rotamer in which the fluorinated arene is perpendicular to the plane of the pyridazine. The NMR signal assignment for **23** is further evidenced by the presence of through-space ^1H – ^{19}F coupling ($J = 4.0$ Hz), where the proximal bridgehead hydrogen is split by the ortho fluorine of the aromatic ring (Figure 2), a feature previously studied in fluorinated iptycenes.⁴⁷ We also observe through-space ^{13}C – ^{19}F coupling where the proximal bridgehead carbon is split by the ortho fluorine ($J = 4.5$ Hz). These through-space couplings are indicative of the short H–F (2.541 Å) and C–F (2.9965(12) Å) distances imposed by the molecular architecture as revealed in the X-ray structure for **23**, which are shorter than the sum of the van der Waals radii.

In a third series, wherein the pendant arene is a 5- or 6-membered heterocycle devoid of a substituent in at least one ortho position, such as 2-thienyl or 3-pyridazinyl, the bridgehead hydrogen resonance⁴⁸ is shifted downfield. Iptycene-derived pyridazines bearing a 2-thienyl substituent (e.g., **19**, **20**, **25**) experience a dramatic shift (e.g., **5a** \rightarrow **19** $\Delta\delta = +0.43$ to 6.27 ppm) consistent with the hypothesis that a coplanar rotamer is favored. This is also supported by the observation of the same rotamer by X-ray crystallography for **19** (vide supra). Iptycene-derived pyridazine dimers (**31a–c**, **33a–d**, **34**) and higher oligomers (**37**, **38**) also show a similar behavior. The signal assigned to the “internal” bridgehead hydrogens, which are proximal to the second pyridazine ring, are also shifted considerably downfield compared to the “external” bridgehead hydrogens that are proximal to a methoxy group or a halogen. For example, the “internal” bridgehead hydrogen of the dichloro dimer **33a** has a chemical shift of δ 6.37 ppm, while the “external” bridgehead hydrogen resonates at δ 5.99 ppm (Figure 2). Furthermore, spectra of the unsymmetrical dimer (**34**) and the higher oligomers (**37**, **38**) are consistent with the hypothesis that the shift is caused by the ring current anisotropy of an adjacent coplanar arene. The dimer **34** displays two downfield signals above 6.20 ppm and two upfield signals around 6.00 ppm, the tetramer **37** displays three “internal”, downfield signals and one “external”, upfield signal, and finally the hexamer **38** shows five “internal”, downfield signals and one “external”, upfield signal. The extent of this chemical shift difference varies between the different compounds, ranging from $\Delta\delta = +0.07$ to 1.00 ppm. The two highest values ($\Delta\delta = +0.69$ and 1.00 ppm) belong to the symmetrically alkylated dimers **33c** and **31c**, which are expected to greatly favor an antiperiplanar or anticlinal (N–C–C–N) rotamer due to the additional steric clash between the alkyl groups that a synclinal rotamer would incur.

The iptycene-derived phthalazine dimer **35** may not be directly compared to the other molecules of the series, due to the greater distance between the bridgehead hydrogen and the aryl substituent. Parallel conclusions can nonetheless be made on the basis of its ^1H NMR spectrum. The monomers **13a** and **14a** display ^1H NMR signals assigned to the bridgehead hydrogens at 5.79, 5.72, and 5.69 ppm, while the proximal phthalazine hydrogens are assigned to signals at 8.25, 8.16, and

(47) (a) Ōki, M. *Acc. Chem. Res.* **1990**, *23*, 351–356. (b) Yamamoto, G.; Ōki, M. *Tetrahedron Lett.* **1985**, *26*, 457–460. (c) Yamamoto, G.; Ōki, M. *J. Org. Chem.* **1984**, *49*, 1913–1917.

(48) The assignments are confirmed by an NOE enhancement of ortho protons of the 2-thienyl substituents (+9.3–12.1%) upon irradiation of the proximal bridgehead protons. For 3-pyridazinyl substituents, NOE enhancements were observed only between the bridgehead protons and the proximal hydrogens within the iptycene scaffold. See the Supporting Information for details.

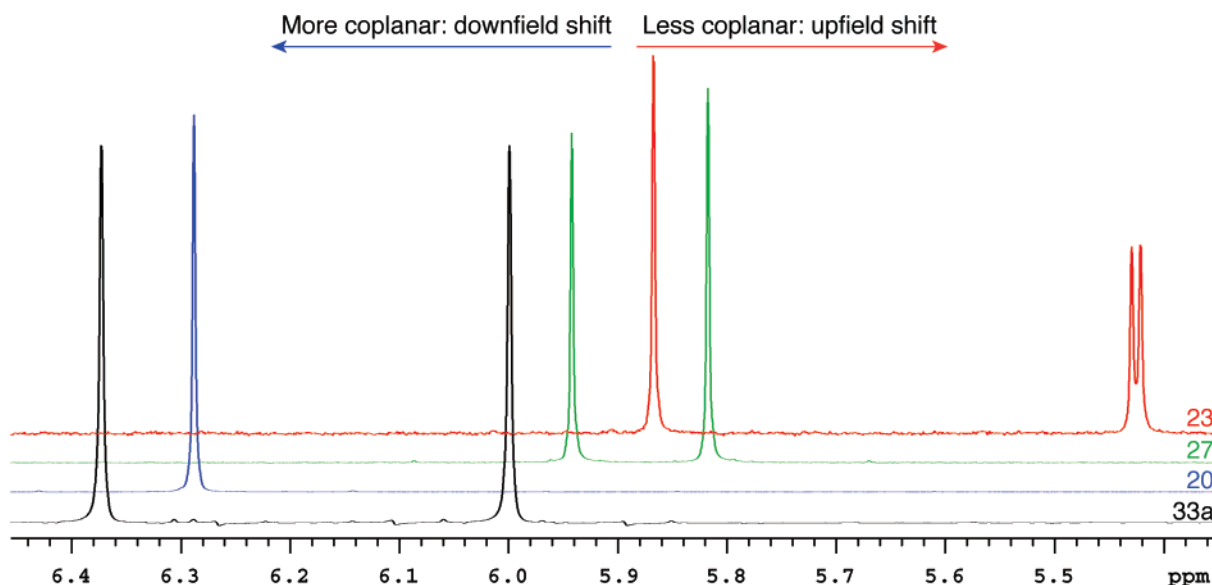


FIGURE 2. Comparative ^1H NMR spectra of the iptycene bridgehead region illustrating the shifts experienced by hydrogens that are proximal to a coplanar arene (**20**, **33a** “internal” H) and by the hydrogens that are proximal to an oblique (**27**) or perpendicular (**23**) arene.

8.13 ppm. In the dimeric iptycene-derived phthalazine **35**, the corresponding signals are observed at 8.29, 7.82, 5.67, and 5.45 ppm. On the basis of these assignments, and under the assumption that the signals that experience the more dramatic shifts correspond to the internal protons of the dimer,⁴⁹ it appears that a significant shielding occurs for both the internal bridgehead hydrogen ($\Delta\delta = -0.24$ ppm) and the internal phthalazine hydrogen ($\Delta\delta = -0.31$ ppm). Thus, we conclude that the preferred (or averaged) rotamer of **35** is not synperiplanar but instead oblique or perpendicular, as for **23**.

(c) Modeling. To further support the hypothesis that coplanarization and conjugation may be favored or at the minimum less disfavored in aryl-substituted, iptycene-derived, pyridazine- or phthalazine-based molecular materials, *ab initio* calculations were performed as follows.⁵⁰ Molecular geometries (gas phase) were first minimized with the B3LYP functional and the 6-31G+(d,p) basis set (6-31G(d,p) for the iptycene dimers). The energies of the rotamers about the biaryl linkage were then individually calculated every 5° with the B3LYP functional and the 6-31G+(d,p) basis set, and the energy of the coplanar rotamer is reported relative to that of the minimum energy

(49) NOE enhancements between bridgehead protons and proximal iptycene and phthalazine hydrogens allow for the identification of two sets of signals that face either inward or outward from the dimer **35**. The actual assignment of each of these sets to either the “internal” or “external” face must, however, rely on a chemical shift argument.

(50) Calculations were performed using the Gaussian 03 software package: Frisch, M. J.; Trucks, G. W.; Schlegel, H. B.; Scuseria, G. E.; Robb, M. A.; Cheeseman, J. R.; Montgomery, J. A., Jr.; Vreven, T.; Kudin, K. N.; Burant, J. C.; Millam, J. M.; Iyengar, S. S.; Tomasi, J.; Barone, V.; Mennucci, B.; Cossi, M.; Scalmani, G.; Rega, N.; Petersson, G. A.; Nakatsuji, H.; Hada, M.; Ehara, M.; Toyota, K.; Fukuda, R.; Hasegawa, J.; Ishida, M.; Nakajima, T.; Honda, Y.; Kitao, O.; Nakai, H.; Klene, M.; Li, X.; Knox, J. E.; Hratchian, H. P.; Cross, J. B.; Bakken, V.; Adamo, C.; Jaramillo, J.; Gomperts, R.; Stratmann, R. E.; Yazyev, O.; Austin, A. J.; Cammi, R.; Pomelli, C.; Ochterski, J. W.; Ayala, P. Y.; Morokuma, K.; Voth, G. A.; Salvador, P.; Dannenberg, J. J.; Zakrzewski, V. G.; Dapprich, S.; Daniels, A. D.; Strain, M. C.; Farkas, O.; Malick, D. K.; Rabuck, A. D.; Raghavachari, K.; Foresman, J. B.; Ortiz, J. V.; Cui, Q.; Baboul, A. G.; Clifford, S.; Cioslowski, J.; Stefanov, B. B.; Liu, G.; Liashenko, A.; Piskorz, P.; Komaromi, I.; Martin, R. L.; Fox, D. J.; Keith, T.; Al-Laham, M. A.; Peng, C. Y.; Nanayakkara, A.; Challacombe, M.; Gill, P. M. W.; Johnson, B.; Chen, W.; Wong, M. W.; Gonzalez, C.; Pople, J. A. *Gaussian 03*, revision C.02; Gaussian, Inc.: Wallingford, CT, 2004.

conformation. Calculations were also performed on a series of model compounds for the purpose of comparison, and the results are summarized in Table 2. While these results do not necessarily provide an accurate estimate of the barrier to atropisomerization,⁵¹ they provide a means of comparison and facilitate the investigation of structure–property relationships with respect to the ease of coplanarization. The bipyridazine **A** illustrates the working hypothesis for coplanarization, and favors a coplanar and flat conformation with an antiperiplanar (transoid) orientation with respect to the torsion angle formed by the N–C–N atoms of the biaryl junction. A second local energy minimum, which is 8 kcal/mol less stable, that parallels the preferred rotamer of biphenyl **B** is found between 45° and 50° . The iptycene-derived pyridazine dimers (**31a** and **33a**) do not minimize in a perfectly coplanar structure. The iptycene bridgehead hydrogen creates a slight steric clash, resulting in a coplanar rotamer that is less stable by 3–4 kcal/mol, a value comparable to the barrier to rotation about the C–C bonds of substituted or branched alkanes. The torsion angle at the energy minimum is of $\sim 145^\circ$, a value greater than that observed in the crystal structures of **31a** and **33a**, but approaching those found in the crystal structure of **37**. We take this to be additional evidence that the preferred conformation of these molecules in a free or solvated state is more coplanar than in the crystal. It is noteworthy that the relative energy of the coplanar rotamer remains lower than in the analogous pyridazine bearing an *o*-methyl group (**F**, 6 kcal/mol) or than in the corresponding biphthalazine (**H**, 8 kcal/mol), and this fact is attributed to the “tying back” of the bridgehead hydrogen within the iptycene scaffold. The relative energy of the coplanar rotamer is also far lower than in molecules with one (**22**, 20 kcal/mol; **23**, 25 kcal/mol) or two (**J**, 53 kcal/mol; **K**, 83 kcal/mol) of the pyridazine rings replaced by the corresponding aromatic hydrocarbon. A

(51) (a) The calculated barrier to rotation about the C–C biaryl linkage does not account for other molecular motion (torsion, stretching, bending, etc.) that, when combined with rotation, can provide additional lower energy pathways to atropisomeric inversion. As an illustration, the calculated barrier for rotation about the biaryl axis of binaphthyl **L** is of ~ 128 kcal/mol, while the experimental value is of 23.5 kcal/mol (ref 51b). (b) Eliel, E. L.; Wilen, S. H.; Mander, L. N. *Stereochemistry of Organic Compounds*; Wiley-Interscience: New York, 1999, and references therein.

TABLE 2. Computational Modeling Results (B3LYP 6-31G+(d,p)^{50,51}

Dihedral ^a	180.0°	29.9°	40.4°	144.5°	145.2°
E _{rel} ^b	0°	0.5	2.4	3.5	3.7
Dihedral	31.6°	45.2°	132.4°	60.4°	137.1°
E _{rel}	3.8	4.7	6.2	6.8	7.4
Dihedral	132.2°	45.7°	129.8°	65.2°	89.0°
E _{rel}	8.1	20.2	24.6	30.2	53.1
Dihedral	107.7°	74.8°	66.9°		
E _{rel}	82.9	127.7	125.8		

^a Dihedral angle at energy minimum. ^b Relative energy of the coplanar rotamer with respect to that of the minimum energy conformation, in kcal/mol. ^c Energy minimum.

significant lowering of the relative energy of the coplanar rotamer is also encountered with 2-thienyl substituents, as corroborated by X-ray crystal structures and NMR spectroscopy. The relative energy of the coplanar rotamer is no more than 4 kcal/mol less stable for **D**, while for the analogous 2-thienyl arene **G** the difference is 7 kcal/mol. The difference remains lower in the unsubstituted 2-phenylthiophene **B** (0.6 kcal/mol), paralleling that observed between **33a** (or **31a**) and **C**. Significant reduction of the relative energy of the coplanar conformer is also present in the bi(phthalazines) (**H**, 8 kcal/mol; **35**, 7 kcal/mol) relative to the hydrocarbon analogues (**L**, 128 kcal/mol; **M**, 126 kcal/mol).

(d) UV–Vis and IR Spectroscopy. We have postulated the possibility of a stabilizing hydrogen-bonding interaction between the bridgehead hydrogen and a proximal heteroatom. A close inspection of the infrared spectra of a selection of the compounds⁵² did not reveal evidence for these types of interactions. Given that neither computational modeling nor crystallography indicates such an interaction, we conclude that the involvement of hydrogen bonding is at best a very small stabilizing effect. Biaryls and oligoaryls in which coplanar rotamers are favored generally exhibit extended π -conjugation. In oligo *p*-phenylenes, the extended conjugation caused by the addition of aryl rings results in a bathochromic shift of the absorption maxima and in an increase of the molar absorptivity.⁵³ This situation is, however, not paralleled in the iptycene-derived pyridazine oligomers,⁵⁴ suggesting that the less polarizable pyridazine rings

display less efficient electron delocalization. Furthermore, the fact that most of the new compounds presented herein are nonfluorescent⁵⁵ also supports a lack of efficient electron delocalization.⁵⁶ Hence, there would appear to be a minimal electronic driving force for planarization.

Conclusions

In conclusion, we have reported a practical, scalable synthesis of attractive heterocyclic iptycene building blocks. These methods permit the introduction of solubilizing groups, the general application of cross-coupling reactions for the preparation of (het)aryl-substituted iptycene-derived 1,2-diazines, and finally the access to dimers and higher oligomers through reductive couplings. The relaxation of steric hindrance at the ortho positions is supported by crystallographic, spectroscopic, and computational studies. The incorporation of these building blocks as structural components of traditional and conjugated polymers and their use as cyclometalating ligands for transition metals are the object of ongoing research.

Experimental Section

Typical Procedures for the Preparation of the Monomeric Pyridazines (“a” series): (a) **9,10-Dihydro-9,10-etheno-11,12-anthracenedicarboxylic Acid, Cyclic Hydrazide (4a).** Crystals

(54) See the Supporting Information for details.

(55) With the notable exception of the thiophene derivatives (e.g., **19** and **20**) that are strongly fluorescent (see ref 16d).

(56) Edelmann, M. J.; Raimundo, J.-M.; Utesch, N. F.; Diderich, F.; Boudon, C.; Gisselbrecht, J.-P.; Gross, M. *Helv. Chim. Acta* **2002**, *85*, 2195–2213.

(52) See the Supporting Information for details.

(53) Matsuoka, S.; Fujii, H.; Yamada, T.; Pac, C.; Ishida, A.; Takamuku, S.; Kusaba, M.; Nakashima, N.; Yanagida, S.; Hashimoto, K.; Sakata, T. *J. Phys. Chem.* **1991**, *95*, 5802–5808.

of anhydride **3a** (41.1 g, 150 mmol) were crushed in a mortar, and then added to a refluxing solution of $\text{NH}_2\text{NH}_2\cdot\text{HCl}$ (23 g, 336 mmol) in AcOH (800 mL). The resulting mixture is refluxed overnight to yield a colorless, clear solution. The reaction mixture is cooled, and poured into ca. 3 L of H_2O . The resulting precipitate is filtered and dried under reduced pressure to yield **4a** as a white solid (43.6 g, 100%). Mp $>330^\circ\text{C}$; ^1H NMR (500 MHz, $(\text{CD}_3)_2\text{SO}$) δ 11.99 and 11.40 (2 br, 2H), 7.54–7.51 (dd, 4H, $J = 5.3, 3.2$ Hz), 7.06–7.03 (dd, 4H, $J = 5.4, 3.2$ Hz), 5.85 (s, 2H); ^{13}C NMR (125 MHz, $(\text{CD}_3)_2\text{SO}$) δ ~ 157 (br) and ~ 150 (br) and ~ 147 (br) (C=O tautomers in solution), 144.0, 125.4, 124.4, 47.2; IR (KBr) 3435, 3069, 1642, 718; HR-MS (ESI) calcd for $\text{C}_{18}\text{H}_{12}\text{N}_2\text{O}_2$ $[\text{M} + \text{H}]^+$ 289.0972, found 289.0978.

(b) **1,4-Dichloro-9,10-dihydro-9,10-[1',2']benzo-2,3-diazaanthracene (5a)**. Cyclic hydrazide **4a** (11.52 g, 40 mmol) was refluxed overnight in neat POCl_3 (125 mL). The mixture was cooled, and the excess POCl_3 was evaporated under reduced pressure. The brown gummy residue was redissolved in PhMe (ca. 100 mL), and evaporated again under reduced pressure to eliminate more of the residual POCl_3 . The residue was then dissolved in CH_2Cl_2 (ca. 200 mL), triturated with neutral alumina for 1 h, filtered over a neutral alumina plug, and eluted first with CH_2Cl_2 , then with EtOAc. Evaporation of the solvents under reduced pressure yields **5a** as an off-white solid (11.19 g, 86%). Mp $227\text{--}228^\circ\text{C}$; ^1H NMR (500 MHz, CDCl_3) δ 7.56–7.54 (dd, 4H, $J = 5.4, 3.2$ Hz), 7.15–7.13 (dd, 4H, $J = 5.4, 3.2$ Hz), 5.84 (s, 2H); ^{13}C NMR (75 MHz, CDCl_3) δ 151.5, 147.4, 142.0, 126.8, 125.2, 50.4; IR (KBr) 3072, 3050, 2987, 1528, 1459, 1308, 1195; HR-MS (EI) calcd for $\text{C}_{18}\text{H}_{10}\text{Cl}_2\text{N}_2$ $[\text{M}]^+$ 324.0221, found 324.0216.

(c) **1-Chloro-9,10-dihydro-4-methoxy-9,10-[1',2']benzo-2,3-diazaanthracene (6a)**. In a septum-capped Schlenk flask is placed the dichloride **5a** (11.00 g, 33.8 mmol) and solid, dry NaOMe (2.38 g, 44.1 mmol). The flask is evacuated and back-filled with argon five times, and dry tetrahydrofuran (ca. 200 mL) is then added. The resulting mixture is rapidly stirred at room temperature for ca. 22 h, after which TLC indicates complete consumption of the starting material. The cloudy reaction mixture is poured in sat. NaHCO_3 (ca. 150 mL). The organic phase is separated, and the aqueous layer is extracted with three portions of ethyl acetate (ca. 50 mL). The combined organic layers are washed with brine, dried over anhydrous magnesium sulfate, and filtered. Evaporation of the solvents under reduced pressure yields **6a** a fluffy white solid (10.72 g, 99%). Mp $181\text{--}183^\circ\text{C}$; ^1H NMR (500 MHz, CDCl_3) δ 7.50–7.47 (m, 4H), 7.09–7.07 (m, 4H), 5.79 (d, 2H), 4.16 (s, 3H); ^{13}C NMR (125 MHz, CDCl_3) δ 160.7, 147.7, 147.5, 143.1, 143.0, 138.1, 126.2, 126.1, 124.9, 124.8, 55.4, 50.5, 47.2; IR (KBr) 3045, 2949, 1568, 1458, 1305, 1208, 730; HR-MS (ESI) calcd for $\text{C}_{19}\text{H}_{13}\text{ClN}_2\text{O}$ $[\text{M} + \text{H}]^+$ 321.0789, found 321.0790.

(d) **1,1,4,4,8,8,11,11-Octamethyl-1,2,3,4,8,9,10,11-octahydro-pentacene (8)**. 9,10-Dihydroanthracene (27 g, 150 mmol) and 2,5-dichloro-2,5-dimethylhexane (75 g, 410 mmol) were placed in a 1-L Schlenk flask, and the contents were evacuated and back-filled with argon five times. Dry CH_2Cl_2 (ca. 600 mL) was added to the flask and the resulting solution was then cooled to -78°C in a dry ice/acetone bath, at which point the contents turned into a loose sludge or slurry. To the reaction mixture was then slowly added TiCl_4 (86 g, 450 mmol) over the course of ca. 10–20 min. The reaction mixture was stirred overnight as it was allowed to slowly warm to room temperature. As the reaction progresses gases (presumably HCl) are slowly evacuated through a connection to an oil bubbler. The contents of the reaction mixture were poured over crushed ice (~ 600 mL) and extracted with CH_2Cl_2 . The combined organic layers were washed with sat. NaHCO_3 and dried over MgSO_4 and the solvent was evaporated under reduced pressure. The crude solid was purified by passage through a SiO_2 plug first with hexanes, then with CH_2Cl_2 as eluant. After evaporation of the solvents the resulting solid was further purified by suspending and triturating in boiling EtOH (ca. 1.5 L). After isolation by filtration and drying under vacuum, the anthracene **8** is obtained as a pale

yellow solid (50.9 g, 85% over two crops). Mp $255\text{--}256^\circ\text{C}$; ^1H NMR (300 MHz, CDCl_3) δ 8.21 (s, 2H), 7.90 (s, 4H), 1.81 (s, 8H), 1.45 (s, 24H); ^{13}C NMR (75 MHz, CDCl_3) δ 143.8, 130.7, 124.7, 123.9, 35.3, 34.9, 32.9; HR-MS (EI) calcd for $\text{C}_{30}\text{H}_{38}$ $[\text{M}]^+$ 398.2968, found 398.2973.

Typical Procedures for the Preparation of Monomeric Phthalazines (“a” series): (a) 9,10-Dihydro-9,10-[1',2']benzoanthracene-2,3-dicarboxylic Acid, Cyclic Hydrazide (12a). Anhydrous hydrazine (6.0 mL, ca. 190 mmol) was added to a refluxing solution of phthalate **11a** (4.50 g, 12 mmol) in EtOH (60 mL) under a nitrogen atmosphere. The resulting mixture was then refluxed overnight. After cooling to room temperature and evaporation of the solvents under reduced pressure, trituration of the crude product in water followed by filtration and drying under vacuum yields the cyclic hydrazide **12a** as a white solid (4.03 g, 98%). Mp $>330^\circ\text{C}$; ^1H NMR (500 MHz, $(\text{CD}_3)_2\text{SO}$) δ 8.12 (s, 2H), 7.51–7.49 (dd, 4H, $J = 8.5, 5.5$ Hz), 7.05–7.04 (dd, 4H, $J = 5.5, 3.5$ Hz), 5.95 (s, 2H); ^{13}C NMR (125 MHz, $(\text{CD}_3)_2\text{SO}$) δ 155.6, 149.1, 144.2, 125.7, 125.5, 124.1, 119.8, 52.4; HR-MS (ESI) calcd for $\text{C}_{22}\text{H}_{14}\text{N}_2\text{O}_2$ $[\text{M} + \text{H}]^+$ 339.1128, found 339.1118.

(b) **1,4-Dichloro-6,11-dihydro-6,11-[1',2']benzo-2,3-diaza-tetracene (13a)**. Cyclic hydrazide **12a** (3.38 g, 10 mmol) was refluxed overnight in neat POCl_3 (35 mL). After the solution was cooled to room temperature, the excess POCl_3 was evaporated under reduced pressure and the residue was redissolved in ca. 35 mL of PhMe. Solvents were again evaporated under reduced pressure, and the residue was dissolved in CH_2Cl_2 (~ 100 mL). A few grams of neutral alumina was added, and the resulting suspension was triturated for 1 h. The contents were then passed through an alumina plug and eluted first with CH_2Cl_2 , then EtOAc. Evaporation of the solvents yields the crude dichloride, which may be further purified by column chromatography on SiO_2 with use of progressively more polar 15:4:1 \rightarrow 10:4:1 hexanes:dichloromethane:ethyl acetate (v/v/v) as the mobile phase to yield **13a** as a yellow solid (1.86 g, 50%). Mp 330°C dec; ^1H NMR (500 MHz, CDCl_3) δ 8.25 (s, 2H), 7.53–7.51 (dd, 4H, $J = 5.0, 3.0$ Hz), 7.12–7.10 (dd, 4H, $J = 5.5, 3.5$ Hz), 5.79 (s, 2H); ^{13}C NMR (125 MHz, CDCl_3) δ 154.8, 151.9, 142.8, 126.5, 126.1, 124.5, 119.7, 54.0; HR-MS (ESI) calcd for $\text{C}_{22}\text{H}_{12}\text{N}_2\text{Cl}_2$ $[\text{M} + \text{Na}]^+$ 397.0270, found 397.0271.

(c) **1-Chloro-6,11-dihydro-4-methoxy-6,11-[1',2']benzo-2,3-diaza-tetracene (14a)**. Dichloride **13a** (750 mg, 2.0 mmol) and solid NaOMe (140 mg, 2.6 mmol) were placed in a Schlenk flask, and the contents were evacuated and back-filled with argon five times. Dry THF (10 mL) was added and the resulting mixture was stirred at room temperature overnight. The reaction mixture was then dumped in an excess of sat. NaHCO_3 , and extracted with EtOAc. The combined organic layers were washed with brine and dried with MgSO_4 , and the solvents were evaporated under reduced pressure to yield a crude product that was purified by column chromatography on SiO_2 with use of progressively more polar 15:4:1 \rightarrow 10:4:1 hexanes:dichloromethane:ethyl acetate (v/v/v) to afford **14a** as an off-white solid (559 mg, 76%). Mp 289°C dec; ^1H NMR (500 MHz, CDCl_3) δ 8.16 (s, 1H), 8.13 (s, 1H), 7.50–7.46 (dq, 4H), 7.09–7.07 (m, 4H), 5.72 (s, 1H), 5.69 (s, 1H), 4.23 (s, 3H); ^{13}C NMR (125 MHz, CDCl_3) δ 160.9, 150.4, 150.1, 143.40, 143.39, 126.3, 126.2, 124.4, 124.3, 119.9, 119.3, 117.7, 55.3, 54.2, 54.1; HR-MS (ESI) calcd for $\text{C}_{23}\text{H}_{15}\text{ClN}_2\text{O}$ $[\text{M} + \text{H}]^+$ 371.0946, found 371.0943.

Typical Procedure for Cross-Coupling Reactions: 9,10-Dihydro-1-methoxy-4-phenyl-9,10-[1',2']benzo-2,3-diazaanthracene (22). In a Schlenk flask were added the methoxy chloride **6a** (3.00 g, 9.35 mmol), $\text{PhB}(\text{OH})_2$ (2.1 g, 17.2 mmol), CsF (4.6 mg, 30 mmol), and $\text{Pd}(\text{PPh}_3)_4$ (600 mg, 0.52 mmol). The flask was evacuated and back-filled with argon five times, then dry dioxane (25 mL) was added. The solution was stirred at 115°C for 48 h. After cooling to room temperature, the reaction mixture was passed on a SiO_2 plug and eluted with EtOAc. Evaporation of the solvents yields a crude product that was purified by column chromatography on SiO_2 with use of progressively more polar 90:10 \rightarrow 75:25

hexanes:ethyl acetate (v/v) to afford **22** as a white solid (3.09 g, 91%). Mp 213–215 °C; ¹H NMR (500 MHz, CDCl₃) δ 7.72–7.70 (d, 2H, *J* = 7.0 Hz), 7.63–7.60 (t, 2H, *J* = 7.3 Hz), 7.58–7.56 (d, 1H, *J* = 7.0 Hz), 7.53–7.52 (d, 2H, *J* = 6.5 Hz), 7.42–7.40 (d, 2H, *J* = 6.0 Hz), 7.10–7.04 (m, 4H), 5.90 (s, 1H), 5.81 (s, 1H), 4.20 (s, 3H); ¹³C NMR (125 MHz, CDCl₃) δ 160.1, 153.8, 147.1, 143.85, 143.79, 136.6, 135.2, 129.4, 129.0, 128.9, 126.0, 125.9, 124.8, 124.5, 55.1, 50.4, 46.8; IR (KBr) 3043, 2945, 1570, 1458, 1315, 1265, 736; HR-MS (ESI) calcd for C₂₅H₁₈N₂O [M + H]⁺ 363.1492, found 363.1485.

Typical Procedures for the Preparation of Dimers and Higher Oligomers by Reductive Coupling (“a” series): (a) **1,1'-Bi(9,10-dihydro-4-methoxy-9,10-[1'',2'']benzeno-2,3-diazaanthracenyl) (31a)**. In a septum-capped Schlenk flask are placed the methoxy chloride **6a** (7.50 g, 23 mmol), activated zinc dust (9.1 g, 140 mmol), *trans*-dichlorobis(triphenylphosphine)palladium(II) (820 mg, 1.2 mmol), and triphenylphosphine (612 mg, 2.3 mmol). The flask is evacuated and back-filled with argon five times, and dry dimethylformamide (ca. 90 mL) is added. The resulting mixture is stirred at 100 °C for ca. 20 h, after which TLC indicates complete consumption of the starting material. The reaction mixture is then poured into a large excess of aq Na₂EDTA and triturated for a few hours. Filtration of the precipitates yields a crude product that is purified by column chromatography on silica gel with use of 10:4:1 hexanes:dichloromethane:ethyl acetate (v/v/v) as the mobile phase, to yield the pure **31a** as a white solid (6.34 g, 95%). Mp >330 °C; ¹H NMR (500 MHz, CDCl₃) δ 7.52–7.50 (d, 4H, *J* = 7 Hz), 7.41–7.40 (d, 4H, *J* = 7 Hz), 7.07–6.99 (m, 8H), 6.14 (s, 2H), 5.93 (s, 2H), 4.36 (s, 6H); ¹³C NMR (125 MHz, CDCl₃) δ 160.6, 150.2, 149.4, 144.2, 143.7, 136.2, 126.0, 125.7, 125.4, 124.4, 55.4, 50.2, 46.8; IR (KBr) 3044, 2949, 1568, 1457, 1347, 1263, 729; HR-MS (ESI) calcd for C₃₈H₂₆N₄O₂ [M + H]⁺ 571.2129, found 571.2122.

(b) **1,1'-Bi(9,10-dihydro-9,10-[1'',2'']benzeno-2,3-diazaanthracenyl)-4,4'(3*H*,3'*H*)-dione (32a)**. Dimethoxy dimer **31a** (6.00 g, 10.5 mmol) was added to a stirred solution of hydrogen bromide in acetic acid (33% by wt, 60 mL) and the mixture was heated to 90 °C overnight. Upon warming dissolution occurs and a violent gas release is observed. The mixture is then cooled and most of the solvent is evaporated under reduced pressure. The resulting solid is suspended and triturated for several hours in a solution of sodium acetate (ca. 25 g in 200 mL of H₂O). Filtration affords **32a** as a pale beige solid (5.20 g, 91%). Mp >330 °C; ¹H NMR (500 MHz, (CD₃)₂SO) δ 13.59 (s, 2H), 7.56–7.55 (d, 4H, *J* = 7 Hz), 7.39–7.38 (d, 4H, *J* = 7 Hz), 7.00–6.99 (m, 8H), 6.03 (s, 2H), 5.98 (s, 2H); ¹³C NMR (125 MHz, (CD₃)₂SO) δ 158.3, 150.4, 146.3, 143.9, 143.7, 138.4, 125.4, 124.8, 124.2, 49.7, 46.4; HR-MS (ESI) calcd for C₃₆H₂₂N₄O₂ [M + H]⁺ 543.1816, found 543.1838.

(c) **1,1'-Bi(4-chloro-9,10-dihydro-9,10-[1'',2'']benzeno-2,3-diazaanthracenyl) (33a)**. The deprotected dimer **32a** (4.00 g, 74 mmol) was stirred overnight at 90 °C in ca. 80 mL of neat POCl₃. The mixture was cooled, and the excess POCl₃ was evaporated under reduced pressure. The brown gummy residue was redissolved in PhMe (ca. 50 mL) and evaporated again under reduced pressure to eliminate more of the residual POCl₃. The residue was then dissolved in CH₂Cl₂ (ca. 80 mL), triturated with neutral alumina for 1 h, filtered through a neutral alumina plug, and eluted first with CH₂Cl₂, then with EtOAc. Evaporation of the solvents under reduced pressure, followed by purification by chromatography on SiO₂ with use of 10:4:1 hexanes:dichloromethane:ethyl acetate (v/v/v) as the mobile phase yields the pure **33a** as a white solid (2.84 g, 66%). Mp >330 °C; ¹H NMR (500 MHz, CDCl₃) δ 7.58–7.56 (d, 4H, 7 Hz), 7.49–7.48 (d, 4H, 7 Hz), 7.13–7.06 (m, 8H), 6.37 (s, 2H), 5.99 (s, 2H); ¹³C NMR (75 MHz, CDCl₃) δ 152.4, 151.8, 149.2, 146.6, 142.9, 142.4, 126.6, 126.4, 125.7, 124.9, 50.20, 50.17; IR (KBr) 3044, 2988, 1531, 1459, 1287, 1194, 705; HR-MS (ESI) calcd for C₃₆H₂₀Cl₂N₄ [M + H]⁺ 579.1138, found 579.1117.

(d) **6-Chloro-4,4',5,5'-bis(9,10-dihydroanthracen-9,10-diyl)-6'-methoxy-3,3'-bipyridazine (34)**. Dichloro dimer **33a** (1.16 g,

2.0 mmol) and solid NaOMe (125 mg, 2.3 mmol) were placed in a Schlenk flask, and the contents were evacuated and back-filled with argon five times. Dry THF (~50 mL) was added and the resulting mixture was stirred at room temperature for 2 days. Solvents were then evaporated under reduced pressure and the residue was purified by chromatography on SiO₂ with use of 10:4:1 hexanes:dichloromethane:ethyl acetate (v/v/v) as the mobile phase to yield first unreacted starting material **33a** (0.48 g recovery), followed by the desired chloro methoxy dimer **34** as a white solid (0.32 g, 28% or 47% based on recovered starting material) and finally the dimethoxy dimer **31a** (0.10 g). Mp 318 °C dec; ¹H NMR (500 MHz, CDCl₃) δ 7.59–7.57 (d, 2H, *J* = 7.0 Hz), 7.54–7.53 (d, 2H, *J* = 7.0 Hz), 7.51–7.50 (d, 2H, *J* = 7.0 Hz), 7.45–7.44 (d, 2H, *J* = 7.0 Hz), 7.14–7.02 (m, 8H), 6.40 (s, 1H), 6.23 (s, 1H), 6.01 (s, 1H), 5.96 (s, 1H), 4.36 (s, 3H); ¹³C NMR (125 MHz, CDCl₃) δ 160.8, 152.7, 151.9, 149.8, 149.3, 148.8, 146.3, 143.9, 143.5, 143.1, 142.5, 136.5, 126.5, 126.2, 126.0, 125.8, 125.7, 125.4, 124.8, 124.5, 55.5, 50.3, 50.2, 50.0, 46.7; HR-MS (ESI) calcd for C₃₇H₂₃ClN₄O [M + H]⁺ 575.1633, found 575.1613.

(e) **1,1'-Bi(6,11-dihydro-4-methoxy-6,11-[1'',2'']benzeno-2,3-diazatetracenyl) (35)**. In a septum-capped Schlenk flask are placed the methoxy chloride **14a** (185 mg, 0.5 mmol), activated zinc dust (195 mg, 3.0 mmol), *trans*-dichlorobis(triphenylphosphine)palladium(II) (35 mg, 0.05 mmol), and triphenylphosphine (26 mg, 0.10 mmol). The flask is evacuated and back-filled with argon five times, and dry dimethylformamide (3 mL) is then added. The resulting mixture is stirred at 100 °C for ca. 20 h, after which TLC indicates complete consumption of the starting material. The reaction mixture is poured into a large excess of aq Na₂EDTA and triturated for a few hours. Filtration of the precipitates yields a crude product that is purified by column chromatography on silica gel with use of 5:1 dichloromethane:ethyl acetate (v/v) as the mobile phase, yielding the pure dimer **35** as a white solid (37 mg, 17%). Mp >310 °C dec; ¹H NMR (500 MHz, CDCl₃) δ 8.29 (s, 2H), 7.82 (s, 2H), 7.44–7.42 (d, 4H, *J* = 6.5 Hz), 7.32–7.31 (d, 4H, *J* = 7.0 Hz), 7.05–6.97 (m, 8H), 5.67 (s, 2H), 5.45 (s, 2H), 4.38 (s, 6H); ¹³C NMR (125 MHz, CDCl₃) δ 161.0, 152.4, 149.3, 149.1, 143.58, 143.55, 127.6, 126.04, 126.03, 124.5, 124.1, 120.4, 118.8, 117.1, 55.3, 54.2, 53.9; HR-MS (ESI) calcd for C₄₆H₃₀N₄O₂ [M + H]⁺ 671.2442, found 671.2446.

(f) **Quaterpyridazine (37)**. In a septum-capped Schlenk flask are placed the chloro methoxy dimer **34** (115 mg, 0.20 mmol), activated zinc dust (78 mg, 1.2 mmol), *trans*-dichlorobis(triphenylphosphine)palladium(II) (14 mg, 0.02 mmol), and triphenylphosphine (11 mg, 0.04 mmol). The flask is evacuated and back-filled with argon five times, and dry dimethylformamide (3 mL) is then added. The resulting mixture is stirred at 100 °C for ca. 20 h. After cooling to room temperature, the mixture is diluted with dichloromethane (~5 mL) and SiO₂ (~300 mg) is added. Evaporation of the solvents under reduced pressure affords a crude product dispersed on silica gel that is purified by column chromatography on silica gel with use of progressively more polar 10:4:1 → 5:4:1 hexanes:dichloromethane:ethyl acetate (v/v/v) as the mobile phase, yielding the pure tetramer **37** as a pale yellow solid (82 mg, 79%). Mp >210 °C dec; ¹H NMR (500 MHz, CDCl₃) δ 7.58–7.56 (m, 4H), 7.52–7.50 (m, 4H), 7.46–7.44 (m, 4H), 7.43–7.41 (m, 4H), 7.13–7.07 (m, 16H), 6.41 (s, 2H), 6.18 (s, 2H), 6.09 (s, 2H), 6.01 (s, 2H), 4.44 (s, 6H); ¹³C NMR (125 MHz, CDCl₃) δ 160.9, 152.7, 152.6, 150.3, 150.0, 147.8, 147.4, 144.1, 143.7, 143.5, 143.3, 136.4, 126.3, 126.2, 126.1, 125.9, 125.4, 125.3, 125.2, 124.6, 55.5, 50.5, 50.0, 49.8, 46.9; IR (KBr) 3043, 2951, 1569, 1459, 1379, 1299, 730; HR-MS (ESI) calcd for C₇₄H₄₆N₈O₂ [M + H]⁺ 1079.3816, found 1079.3782.

(g) **Sexipyridazine (38)**. In a septum-capped Schlenk flask are placed the chloro methoxy dimer **34** (230 mg, 0.40 mmol), the dichloro dimer **33a** (58 mg, 0.10 mmol), activated zinc dust (235 mg, 3.6 mmol), *trans*-dichlorobis(triphenylphosphine)palladium(II) (42 mg, 0.06 mmol), and triphenylphosphine (32 mg, 0.12 mmol). The flask is evacuated and back-filled with argon five times,

and dry dimethylformamide (3 mL) is then added. The resulting mixture is stirred at 100 °C for ca. 24 h. After cooling to room temperature, the mixture is diluted with dichloromethane (~5 mL) and SiO₂ (~300 mg) is added. Evaporation of the solvents under reduced pressure affords a crude product dispersed on silica gel that is purified by column chromatography on silica gel with use of progressively more polar 10:4:1 → 5:4:1 hexanes:dichloromethane:ethyl acetate (v/v/v) as the mobile phase, yielding first fractions containing the tetramer **37**, followed by fractions of lower *R_f* containing the hexamer **38**. Further purification by preparative thin layer chromatography on SiO₂ with use of 8:8:2 hexanes:dichloromethane:ethyl acetate (v/v/v) as the mobile phase affords the hexamer **38** as a pale yellow solid (20 mg, 13%) with an estimated purity of 90–95% by NMR that could not be further upped by chromatography or crystallization. Mp >330 °C; ¹H NMR (500 MHz, CDCl₃) δ 7.61–7.57 (m, 4H), 7.56–7.55 (m, 4H), 7.53–7.48 (m, 16H), 7.16–7.11 (m, 24H), 6.45 (s, 2H), 6.24 (s, 2H), 6.22 (s, 2H), 6.21 (s, 2H), 6.17 (s, 2H), 6.04 (s, 2H), 4.47 (s, 6H); ¹³C NMR (125 MHz, CDCl₃) δ 161.0, 153.1, 152.9, 152.8, 152.5, 150.3, 150.0, 148.1, 148.0, 147.9, 147.5, 144.1, 143.8, 143.5, 143.4, 143.3, 136.5, 126.5, 126.4, 126.3, 126.1, 125.9, 125.5, 125.5,

125.4, 125.3, 125.2, 124.6, 55.6, 50.6, 50.1 (3), 49.8, 46.9; IR (KBr) 3042, 2950, 2926, 1570, 1459, 1374, 1297, 729; HR-MS (ESI) calcd for C₁₁₀H₆₆N₁₂O₂ [M + 2H]²⁺ 794.2789, found 794.2773.

Acknowledgment. This work was supported in part by a NSERC fellowship (J.B.), the Office of Naval Research and the National Science Foundation. We thank Dr. Changsik Song for a gift of 2,2'-bithiophen-5-yltributylstannane, and Dr. Phoebe Kwan for a gift of 2-tributylstannyl-3,4-ethylenedioxythiophene. We thank the Department of Chemistry Instrumentation Facility at MIT for HR-MS and NMR assistance.

Supporting Information Available: Complete experimental procedures and characterization data including copies of the ¹H and ¹³C NMR spectra for all new compounds, crystallographic data (in CIF format), Cartesian coordinates of the minimized structures and potential energy curve of rotamers about the biaryl linkage, and UV–vis and IR spectra of selected compounds. This material is available free of charge via the Internet at <http://pubs.acs.org>.

JO702000D